

Global mesozooplankton communities show lower connectivity in deep oceanic layers

Oriol Canals¹, Jon Corell¹, Ernesto Villarino¹, Guillem Chust², Eva Aylagas Martínez¹, Iñaki Mendibil¹, Craig Michell³, Nacho Gonzalez-Gordillo¹, Xabier Irigoien⁴, and Naiara Rodriguez-Ezpeleta²

¹Affiliation not available

²AZTI

³King Abdullah University of Science and Technology

⁴AZTI-Tecnalia

April 3, 2023

Abstract

Mesozooplankton is a key component of the ocean, regulating global processes such as the carbon pump, and ensuring energy transfer from lower to higher trophic levels. Yet, despite the importance of understanding mesozooplankton diversity, distribution and connectivity at global scale to predict the impact of climate change in marine ecosystems, there is still fragmented knowledge. To fill this gap, we applied DNA metabarcoding to mesozooplankton samples collected during the Malaspina-2010 circumnavigation expedition across temperate and tropical oceans from the surface to bathypelagic depths. By conducting a hidden diversity analysis, we highlight the still scarce knowledge on global mesozooplankton diversity and identify the Indian Ocean and the deep sea as the most understudied areas. By analysing mesozooplankton community spatial distribution, we confirm global biogeographical patterns across the temperate to tropical oceans both in the vertical and horizontal gradients. Additionally, we reveal a consistent increase in mesozooplankton beta-diversity with depth, indicating reduced connectivity at deeper layers, and identify a water mass type-mediated structuring of bathypelagic communities, instead of an oceanic basin-mediated as observed at upper layers. This suggests limited dispersal at deep ocean layers, most likely due to weaker currents and lower mixing of water mass types. Overall, our work supports the neutral theory of biodiversity and thus the importance of oceanic currents and barriers in dispersal in shaping global plankton communities, and provides key knowledge for predicting the impact of climate change in the deep-sea.

1 Title: **Global mesozooplankton communities show lower connectivity in deep oceanic**
2 **layers**

3

4 Running title: **Low deep-sea mesozooplankton connectivity**

5

6 Oriol Canals¹, Jon Corell¹, Ernesto Villarino¹, Guillem Chust¹, Eva Aylagas¹, Iñaki Mendibil¹,
7 Craig T. Michell², J.I. González-Gordillo³, Xabier Irigoien^{1,#}, Naiara Rodríguez-Ezpeleta^{1*}

8 ¹AZTI Marine Research Division, Basque Research and Technology Alliance (BRTA),
9 Txatxarramendi ugarte a z/g, E-48395 Sukarrieta, Bizkaia, Spain.

10 ²Biological and Environmental Science and Engineering Division, Red Sea Research Centre,
11 King Abdullah University of Science and Technology, 23955-6900 Thuwal, Kingdom of Saudi
12 Arabia.

13 ³Área de Ecología, Facultad de Ciencias del Mar y Ambientales, Universidad de Cádiz,
14 Campus de Excelencia Internacional del Mar, E-11510 Puerto Real, Spain.

15 * Corresponding author: nrodriguez@azti.es

16 # Present address: Ocean Science and Solutions Applied Research Institute (OSSARI),
17 Education Research and Innovation Foundation, NEOM Base Camp, Building Number: 4758,
18 Zip Code: 49643 NEOM, Saudi Arabia.

19 **Abstract**

20 Mesozooplankton is a key component of the ocean, regulating global processes such as the
21 carbon pump, and ensuring energy transfer from lower to higher trophic levels. Yet, despite
22 the importance of understanding mesozooplankton diversity, distribution and connectivity
23 at global scale to predict the impact of climate change in marine ecosystems, there is still
24 fragmented knowledge. To fill this gap, we applied DNA metabarcoding to
25 mesozooplankton samples collected during the Malaspina-2010 circumnavigation
26 expedition across temperate and tropical oceans from the surface to bathypelagic depths.
27 By conducting a hidden diversity analysis, we highlight the still scarce knowledge on global
28 mesozooplankton diversity and identify the Indian Ocean and the deep sea as the most
29 understudied areas. By analysing mesozooplankton community spatial distribution, we
30 confirm global biogeographical patterns across the temperate to tropical oceans both in the
31 vertical and horizontal gradients. Additionally, we reveal a consistent increase in
32 mesozooplankton beta-diversity with depth, indicating reduced connectivity at deeper
33 layers, and identify a water mass type-mediated structuring of bathypelagic communities,
34 instead of an oceanic basin-mediated as observed at upper layers. This suggests limited
35 dispersal at deep ocean layers, most likely due to weaker currents and lower mixing of water
36 mass types. Overall, our work supports the neutral theory of biodiversity and thus the
37 importance of oceanic currents and barriers in dispersal in shaping global plankton
38 communities, and provides key knowledge for predicting the impact of climate change in
39 the deep-sea.

40 **Keywords:** deep ocean, zooplankton, connectivity, dispersal, oceanic currents,
41 environmental selection.

42 **Introduction**

43 Marine mesozooplankton is comprised of a wide range of functionally, phylogenetically,
44 and morphologically diverse organisms whose size range from 0.2 to 20 mm (Bucklin et al.,
45 2021; Steinberg & Landry, 2017) and which include some of the most abundant animals on
46 Earth, such as copepods or euphausiids (Turner, 2004). Mesozooplankton taxa are key
47 components of marine ecosystems, ensuring energy transfer from lower to higher trophic
48 levels (Zeldis & Décima, 2020) as main predators of producers and primary consumers
49 (Calbet, 2001) and as main food source of a number of organisms, including many relevant
50 commercial fish species (Hays, Richardson, & Robinson, 2005; Turner, 2004). Additionally,
51 many mesozooplankton species perform diel vertical migrations, significantly contributing
52 to trophic connectivity, and are deeply involved in global biogeochemical cycles such as the
53 biological carbon pump through recycling sinking organic matter and enhancing carbon
54 sequestration in the deep ocean (Bode, Koppelman, Teuber, Hagen, & Auel, 2018;
55 Hernández-León et al., 2020; Kelly et al., 2019; Liszka, Manno, Stowasser, Robinson, &
56 Tarling, 2019; Steinberg & Landry, 2017; X. Zhang & Dam, 1997). Specific plankton
57 community composition and trophic networks have been related to the local intensity of
58 the carbon pump (Ducklow, Steinberg, & Buesseler, 2001; Guidi et al., 2016) and thus
59 increasing knowledge on plankton diversity and on how they are spatially distributed and
60 connected along the horizontal and vertical ocean gradients is essential to monitor and
61 predict the impacts derived from climate change or other anthropogenic perturbations
62 (Chiba et al., 2018; Hays et al., 2005; Ratnarajah et al., 2023). Yet, mesozooplankton

63 diversity still has far to go to be fully described (Bucklin et al., 2021), as well as its global
64 structuring and the factors shaping it along the ocean.

65 Global structuring of planktonic groups in the ocean is assumed to be determined by the
66 interaction between dispersal, speciation, drift, and selection (Vellend, 2010). Dispersal
67 refers to organismal transport, and tends to homogenise community composition among
68 sites (i.e., to decrease beta-diversity; see Whittaker (1960)) (Soininen, Lennon, & Hillebrand,
69 2007). Speciation refers to the appearance of new variants and ultimately species and,
70 contrarily to dispersal, contributes to increasing beta-diversity between sites (Casteleyn et
71 al., 2010). On the other hand, drift and selection act at the alpha-diversity level, shaping the
72 relative abundance of the different species in a community and defining the local diversity
73 (Gilbert & Levine, 2017; Hellweger, van Sebille, & Fredrick, 2014). The interaction between
74 these processes typically results in a distance-decay pattern between biological
75 communities, which is represented by an increase in beta-diversity with increasing
76 geographical distance (Nekola & White, 1999). Distance-decay patterns have been reported
77 from microbes to larger plankton (Cermeño, de Vargas, Abrantes, & Falkowski, 2010; Chust,
78 Irigoien, Chave, & Harris, 2013; Villarino et al., 2022; Villarino et al., 2018). Beta-diversity
79 measurements are also a proxy of connectivity between communities (i.e., the rate of
80 migration of individuals and species between two communities) (Giner et al., 2020; Villarino
81 et al., 2018), so that the higher the beta-diversity the less connected the communities are.

82 The primary factors shaping global plankton distribution and community composition
83 patterns are still unclear. Global plankton structuring in the ocean has been largely
84 considered to follow the classical niche differentiation hypothesis (“everything is

85 everywhere but the environment selects"; Hutchinson (1957)), which considers selection as
86 the main factor determining plankton distribution. Recently, the importance of
87 geographical barriers and oceanic currents in shaping plankton community distribution has
88 been further acknowledged (Chust et al., 2017), and the role of drift and barriers to dispersal
89 has been recognised, in line with the neutral theory of biodiversity (Dornelas, Connolly, &
90 Hughes, 2006; Hubbell, 2001; Pueyo, 2006). In the upper oceanic layers, global plankton
91 dispersal and community assembly rules have been related to oceanic currents and
92 environmental factors (Richter et al., 2020; Villarino et al., 2018; Watson et al., 2011), and
93 to other causes such as body size (Villarino et al., 2018). Knowledge on planktonic spatial
94 distribution patterns at deeper layers is even much scarcer than at upper depths (Chust et
95 al., 2017; St. John et al., 2016). The deep ocean is environmentally more homogeneous
96 (Bode et al., 2018; Danovaro, Dell'Anno, & Pusceddu, 2004) and with generally weaker
97 oceanic currents (Reid, 1969, 1994). Hence it is expected that plankton dispersal and spatial
98 patterns of community composition are differently influenced by dispersal and selection
99 than in upper layers, as recently reported for prokaryotes and picoeukaryotes (Giner et al.,
100 2020; Villarino et al., 2022).

101 In the horizontal oceanic gradient, epipelagic mesozooplankton diversity and community
102 composition have been reported to vary latitudinally and to be linked to variations in
103 productivity, temperature, salinity and to phytoplankton community composition (Brandão
104 et al., 2021; Domínguez, Garrido, Santos, & dos Santos, 2017; Ibarbalz et al., 2019; Saporiti
105 et al., 2015; Soviadan et al., 2022), in addition to oxygen concentration at mesopelagic
106 depths (Soviadan et al., 2022). Yet, global horizontal mesozooplankton patterns below the

107 mesopelagic zone remain unexplored. Regarding the vertical oceanic gradient,
108 mesozooplankton communities are known to be strongly structured along the water
109 column, with many species showing a clear preference for specific depths (Fernández de
110 Puellas et al., 2019; Hirai, Tachibana, & Tsuda, 2020; Pearman & Irigoien, 2015; Sommer,
111 Van Woudenberg, Lenz, Cepeda, & Goetze, 2017). Because many mesozooplankton
112 organisms perform vertical migrations (Ohman, 1990) and transport direction is related to
113 depth (Fiksen, Jørgensen, Kristiansen, Vikebø, & Huse, 2007), the resulting distribution
114 pattern of mesozooplankton is a complex combination of such processes together with
115 adaptation to water mass environment, demographic traits and stochasticity.

116 Studies analysing the global distribution and connectivity of mesozooplankton communities
117 and the ecological mechanisms shaping them are limited partly due to the scarcity of
118 globally scaled surveys. Additionally, exploring the deep ocean has added challenges related
119 to the sampling at high depths. To date, most studies on mesozooplankton have been
120 carried out at local (Domínguez et al., 2017; Ershova & Kosobokova, 2019; Kim, Lee, Lee,
121 Oh, & Kim, 2020; Pearman & Irigoien, 2015) or regional (Carlotti et al., 2018; Cheng et al.,
122 2022; Feliú, Pagano, Hidalgo, & Carlotti, 2020; Landry, Hood, & Davies, 2020; Siokou et al.,
123 2019) scales, and only some studies covered large oceanic transects (Bode et al., 2018; Hirai
124 et al., 2020; Vereshchaka, Abyzova, Lunina, & Musaeva, 2017) or global oceanic areas
125 (Fernández de Puellas et al., 2019; Sviadan et al., 2022). Another limitation lies on the
126 taxonomic identification of mesozooplankton being a time-consuming task that greatly
127 depends on often lacking taxonomic expertise and information of the targeted organisms
128 (Hirai & Tsuda, 2015). Thus, many studies only consider abundant crustaceans (mainly

129 copepods) or identify mesozooplankton groups at higher taxonomic levels (Domínguez et
130 al., 2017; Ershova & Kosobokova, 2019; Siokou et al., 2019; Soviadan et al., 2022). Also,
131 some mesozooplankton groups such as gelatinous organisms are usually under sampled or
132 damaged while sampling with traditional methods (i.e., plankton nets), so that they cannot
133 be identified. The combination of these issues has made it difficult to gather knowledge on
134 the structuring and distribution patterns of mesozooplankton on a global scale.

135 Combining global oceanographic surveys and DNA metabarcoding, i.e., large-scale
136 taxonomic identification of complex samples via analysis of one or few orthologous DNA
137 regions (Bucklin, Lindeque, Rodriguez-Ezpeleta, Albaina, & Lehtiniemi, 2016), is a promising
138 approach for plankton research. Applying DNA metabarcoding to plankton virtually
139 overcomes the need of taxonomic expertise, ensures accurate taxonomic classification of
140 organisms difficult to identify (Bucklin et al., 2016; Govindarajan et al., 2021; Hirai & Tsuda,
141 2015) and allows the detection of hidden diversity, i.e., diversity that remains to be
142 discovered, described, and/or sequenced (Lindeque, Parry, Harmer, Somerfield, & Atkinson,
143 2013).

144 Here, we aim to increase the knowledge on mesozooplankton biodiversity, community
145 structuring, and connectivity in the global ocean along both horizontal and vertical oceanic
146 gradients by i) identifying the oceanic regions—both in the vertical and horizontal scales—
147 with a higher amount of hidden diversity and thus needing more taxonomic efforts, ii)
148 testing whether patterns in mesozooplankton alpha- and beta-diversity and community
149 structure differ along the vertical and horizontal gradients at a global oceanic scale, and iii)
150 unveiling the factors determining mesozooplankton spatial distribution and connectivity at

151 different oceanic depths. To achieve these goals, we applied DNA metabarcoding to
152 mesozooplankton samples collected during the Malaspina-2010 circumnavigation
153 expedition (Duarte, 2015) covering a large temperate to tropical oceanic area comprising
154 the Atlantic, Indian and Pacific Oceans, and four depth ranges, including the epipelagic,
155 upper mesopelagic, lower mesopelagic and bathypelagic layers (down to 3000 m depth).
156 We hypothesise: i) that unexplored oceanic regions, such as the deep sea, harbour a higher
157 proportion of hidden mesozooplankton diversity than those from upper layers, ii) that
158 mesozooplankton communities are subjected to vertical and horizontal oceanic gradients
159 at a global scale, which generate global biogeographic patterns, and iii) that
160 mesozooplankton spatial distribution and connectivity differ at the different ocean layers,
161 with higher dissimilarity between deep-sea communities than between communities at
162 upper layers due to the average weaker deep-sea currents compared to surface ones
163 (Manral et al., 2023; Reid, 1994).

164

165 **Material and methods**

166 *Sampling and environmental data collection*

167 Mesozooplankton samples were collected during the Malaspina 2010 circumnavigation
168 expedition (from December 2010 to July 2011; Duarte (2015)) from 43 different stations
169 (Figure 1) using a 0.5 m² Hydrobios MultiNet (300 µm mesh size) programmed to open at
170 regular depths (0–200, 200–500, 500–1000, 1000–2000 and 2000–3000 m depth) from the
171 surface to 3,000 m depth for a total of 133 samples. All samples were collected during

172 daytime (10:00 to 14:00 am local time). Additional details on the sampling and stations can
173 be found in Fernández de Puelles et al. (2019). On the cruise, each net was softly rinsed with
174 filtered seawater to capture all organisms, which were stored in 50 ml flasks filled with
175 absolute ethanol. At each sampling station a Rosette sampling system fitted with a Seabird
176 0911Plus CTD probe was deployed (Duarte, 2015), measuring seawater temperature (°C),
177 conductivity (S/m), salinity (PSU), fluorescence (Seapoint), photosynthetically active
178 radiation (PAR), and oxygen (ml/l) along the water column. Samples were grouped
179 according to their depth range into 0-200 m (epipelagic layer), 200-500 m (upper
180 mesopelagic), 500-1000 m (lower mesopelagic) and 1000-3000 m depth (bathypelagic);
181 when two samples covered a unique depth range, they were pooled after sequencing into
182 one unique integrated sample by summing up their absolute number of reads (i.e., samples
183 collected at 1000-2000 and 2000-3000 m depth were merged into a unique 1000-3000 m
184 sample). Similarly, a unique value of each environmental variable was used for each depth
185 range, which corresponded to the average of all measurements for that depth range (Table
186 S1). It should be noted that we used the term mesozooplankton although the mesh size
187 used for the sampling (300 µm) did not exactly correspond to the size range expected for
188 mesozooplankton (from 200 µm to 2 mm length). This decision responded to the fact that
189 most reads and OTUs corresponded to metazoans that are known to belong to this
190 planktonic fraction.

191 *DNA extraction, quantity, and quality check*

192 Samples were centrifuged (3,500 g; 10 min) to remove ethanol and resulting zooplankton
193 pellets were grinded with a mortar in 1-2 ml lysis buffer (10 mM Tris-HCl, 100 mM EDTA,

194 200 mM NaCl, 1% SDS) until no integer organism could be appreciated. After an overnight
195 incubation with proteinase K (0.2 mg/ml, final concentration) at 56 °C, samples were
196 centrifuged (3,500 g; 15 min) and supernatant was incubated with RNase (37 °C; 30 min).
197 Extracted total DNA was purified using a phenol-chloroform-isoamyl alcohol (25:24:1,
198 vol:vol:vol) mixture followed by ethanol 95% ammonium acetate 0.5 M precipitation. DNA
199 was suspended in 100 µl Milli-Q water and stored at -20 °C until further use. DNA
200 concentration was measured with the Quant-iT dsDNA HS assay kit using a Qubit® 2.0
201 Fluorometer (Life Technologies, California, USA), while DNA purity was inferred from
202 260/280 and 260/230 absorbance ratios with the ND-1000 Nanodrop (Thermo Scientific,
203 Massachusetts, USA). Integrity of extracted genomic DNA was assessed by electrophoresis
204 in 0.7% agarose. Eighteen of the samples did not yield gel-visible DNA.

205 *Library preparation and sequencing*

206 110 samples were amplified using the #1/#2RC primer pair (Machida & Knowlton, 2012)
207 targeting the hypervariable V4 region of the 18S rRNA gene (henceforth *mac18S*) and 85
208 were amplified using the mICOLintF/dgHCO2198 primer pair (Leray et al., 2013) targeting a
209 313 bp length region of the cytochrome oxidase I (COI) gene (henceforth *mICOI*). For the
210 first PCR reaction, 2 µl of genomic DNA (5 ng/µl) were added to a mix consisting of 10 µl of
211 1X Phusion Master Mix (ThermoScientific, Massachusetts, USA), 0.4 µl of each primer (0.2
212 µM) and 7.2 µl of MilliQ water. For the *mICOI* primer pair, annealing was performed for 1
213 min at 46 °C, and for the *mac18S* primer pair annealing was performed for 30 s at 55 °C and
214 only 22 cycles were used. PCR products were purified using AMPure XP beads (Beckman
215 Coulter, California, USA) following manufacturer's instructions and used as templates for

216 the generation of the dual-indexed amplicons in the second PCR reaction following the “16S
217 Metagenomic Sequence Library Preparation” protocol (Illumina, California, USA) using the
218 Nextera XT Index Kit (Illumina, California, USA). Multiplexed PCR products were purified
219 using the AMPure XP beads, quantified using Quant-iT dsDNA HS assay kit using a Qubit®
220 2.0 Fluorometer (Life Technologies, California, USA) and adjusted to 4 nM. Then, 5 µl of
221 each sample were pooled, checked for size and concentration using the Agilent 2100
222 bioanalyzer (Agilent Technologies, California, USA), sequenced using the 2 x 300 paired end
223 protocol on the Illumina MiSeq platform (Illumina, California, USA) and demultiplexed
224 based on their barcode sequences. Four and one samples in *mICOI* and *mac18S*,
225 respectively, produced less than 5,000 reads and were not considered for further analyses.
226 In addition, four and five pairs of samples in *mICOI* and *mac18S*, respectively, belonged to
227 the same depth range and were pooled into unique depth range samples. At the end, the
228 *mICOI* and *mac18S* datasets consisted of a total of 77 and 104 samples (for sample details,
229 see Table S2).

230 *Pre-processing, clustering, and taxonomic assignment of amplicon sequences*

231 The *mICOI* barcode is 313 bp length, while the *mac18S* barcode has a variable length that
232 ranges between 537 to 595 (5 to 95th percentile) in eukaryotes (Figure S1). In order to
233 accommodate these differences, alternative read pre-processing pipelines had to be
234 applied for each marker (Figure S2). In both cases, raw demultiplexed reads were quality
235 checked with FASTQC (<http://www.bioinformatics.babraham.ac.uk/projects/fastqc>). *mICOI*
236 forward and reverse reads were merged using FLASH (Magoč & Salzberg, 2011) with an
237 allowed overlap range of 217 to 257 bp (20 nucleotides more and less of the expected

238 overlap). *mac18S* forward and reverse reads were merged with a minimum overlap of 162,
239 and non-merged pairs were trimmed at 220 bp (based on a median Phred score lower than
240 30 after these positions) and the forward and the reverse complement of the reverse reads
241 were pasted introducing an ambiguous base (N) in between; this was done so that no k-
242 mers including fragments of the forward and reverse reads are used for taxonomic
243 assignment (Jeraldo et al., 2014). Using Trimmomatic (Bolger, Lohse, & Usadel, 2014), for
244 both barcodes only those resulting contigs with a minimum average Phred score of 20 and
245 containing the appropriate primer sequence were retained for subsequent analyses.
246 Sequences with at least one (for *mICOI*) or two (for *mac18S*) ambiguous bases were
247 discarded using mothur (Schloss et al., 2009). Chimeras were detected and removed using
248 UCHIME (Edgar, Haas, Clemente, Quince, & Knight, 2011). Clustering of sequences into
249 operational taxonomic units (OTUs) was performed using SWARM (Mahé, Rognes, Quince,
250 de Vargas, & Dunthorn, 2014) with $d=1$, and singletons (i.e., OTUs with one unique read in
251 the dataset) were removed. Taxonomic assignment was performed according to the naïve
252 Bayesian classifier method from (Wang, Garrity, Tiedje, & Cole, 2007) implemented in
253 mothur against the BOLD (<http://www.boldsystems.org>) and SILVA (release 132) (Quast et
254 al., 2013) databases as references for *mICOI* and *mac18S* barcodes, respectively. For *mICOI*
255 dataset, the sequences assigned to metazoans in the previous step were taxonomically
256 reassigned using the more recent, curated MetaZooGene database (MZGdb) (Bucklin et al.,
257 2021) for a more accurate classification. To compare the results between barcodes, the
258 taxonomic ranks of both databases were adjusted. It should be noted that, in most clades,

259 SILVA database lacked detailed taxonomy for levels below Class, preventing some analyses
260 for the *mac18S* dataset (specified along the manuscript).

261 *Hidden diversity, alpha-, and beta-diversity analyses*

262 To determine the amount of hidden diversity in each oceanic basin and depth layer we
263 relied on the sequence similarity values obtained by comparing the representative
264 sequence of each OTU against the reference sequences in MZGdb using BLAST (Altschul,
265 Gish, Miller, Myers, & Lipman, 1990). To assess horizontal and vertical alpha-diversity
266 patterns we used the OTU richness (number of OTUs) and H index (*diversity* function, *vegan*
267 package version 2.5.6; Oksanen et al. (2019)) measurements.

268 To infer patterns in mesozooplankton community composition similarity and connectivity
269 between sites (beta-diversity), we used Bray-Curtis distances (*vegdist* function, *vegan*
270 package) and phylogenetic community dissimilarities (PCD) (*pcd* function, *picante* package
271 version 1.8.2; Kembel et al. (2010)). For PCD, we only considered the 100 most abundant
272 OTUs due to computational requirements for the analysis. Vertical and horizontal
273 structuring of mesozooplankton communities was examined by applying nonmetric
274 multidimensional scaling (NMDS) (*metaMDS* function, *vegan* package) analysis based on
275 Bray–Curtis and PCD distance matrices, followed by ANOSIM test (Clarke, 1993) (*anosim*
276 function, *vegan* package) to test for statistical significance of communities ordination
277 according to predefined sample groups. Finally, to unveil the factors driving
278 mesozooplankton spatial distribution we relied on the correlations between
279 mesozooplankton community composition distances and environmental and least cost

280 oceanic distances, by using the Mantel test (*mantel* function, *vegan* package).
281 Environmental distances were based on the Euclidean distance (*vegdist* function, *vegan*
282 package) between pairs of sites and included all environmental variables measured after
283 previous standardization to the same scale. The least cost oceanic distances were obtained
284 using the *marmap* package (*lc.dist* function, version 1.0.6; Pante and Simon-Bouhet (2013)).
285 All statistical analyses and plots were conducted in R statistical environment (R version
286 4.0.4; R Core Development Team (2013)).

287

288 **Results**

289 *Global mesozooplankton composition*

290 Most of the *mICOI* and *mac18S* dataset reads and OTUs were assigned to Metazoa, from
291 which over 75% and 100% of both reads and OTUs in *mICOI* and *mac18S*, respectively, were
292 successfully assigned to phylum and used for further analysis (Figure 2a). In both datasets,
293 Arthropoda appeared as the most abundant and diverse group (Figure 2b). Chaetognatha,
294 Cnidaria, Mollusca, Annelida, Vertebrata (Chordata) and Tunicata (Chordata) also exhibited
295 relevant richness and/or abundance in at least one of the datasets. The Class Hexanauplia
296 (Arthropoda), which includes copepods, was the dominant component of the
297 mesozooplankton community in both datasets; other abundant Classes were Malacostraca
298 (Arthropoda; 16.4% and 6.6% of reads in *mICOI* and *mac18S*, respectively), Hydrozoa
299 (Cnidaria; 7.9% and 18.5%) and Actinopterygii (Vertebrata; 6.0% and 1.0%). It should be
300 noted that some taxa were not (or hardly) amplified by one of the markers. For instance,

301 Ostracoda, Chaetognatha and Cephalopoda (Mollusca) were rarely or not detected by
302 *mac18S* despite being relatively abundant in *m/COI* (11.4%, 6.3% and 1.9% of reads,
303 respectively), while Annelida, Gastropoda and Tunicata (Chordata), which represented
304 3.3%, 3.5%, and 8.5% of *mac18S* metazoan reads, respectively, were clearly
305 underrepresented in *m/COI* dataset (0.5%, 0.8%, and 0.02% of reads).

306 At the Class level, mesozooplankton taxonomic composition—and differences in
307 community composition between markers—was overall consistent along the water column
308 (Figure 2b), especially in *mac18S* dataset. Yet, i) an overall trend to increase both the
309 proportion of reads and OTUs assigned to Arthropoda with depth, ii) a peak of Vertebrata
310 reads at lower mesopelagic depths, and iii) a peak of Ostracoda reads and OTUs at the upper
311 mesopelagic layer in the *m/COI* dataset, was observed. Note that these results represent
312 the average taxonomic composition by depth range, and that mesozooplankton community
313 composition differed between sites (Figure S3).

314 Remarkably, just about half of OTUs (representing two thirds of the reads) were successfully
315 assigned to the species level in *m/COI* dataset—analysis not performed in *mac18S* due to
316 SILVA reference database not specifying taxonomic levels below Class. Yet, this percentage
317 greatly varied between and within taxonomic groups (Table S3).

318 *Hidden diversity*

319 We inferred the amount of hidden diversity globally and in the different oceanic basins and
320 depths under study. This inference was based on the sequence similarity values obtained
321 by comparing the representative sequence of each OTU against the reference sequences in

322 MZGdb, i.e., the lower the sequence similarity the farther the retrieved sequence is to an
323 already known (sequenced) organism. The Indian Ocean resulted as the oceanic basin
324 presenting a higher proportion of unknown mesozooplankton diversity (with approximately
325 half of the OTUs displaying less than 90% of sequence similarity to described species),
326 followed by the Pacific and Atlantic basins (Figure 3). In the vertical gradient, we observed
327 a general trend to increase the proportion of hidden diversity with depth (from the
328 epipelagic to mesopelagic and bathypelagic layers) while decreasing the proportion of well-
329 known OTUs (with >98% similarity to MZGdb sequences) below the upper mesopelagic
330 layer. This vertical pattern was observed both globally and at each oceanic basin separately
331 (except for the bathypelagic layer of the Pacific Ocean, whose sequence similarity values
332 were comparable to those from epipelagic depths).

333 *Horizontal and vertical structuring of mesozooplankton community composition*

334 Ordination of communities using NMDS analysis based on Bray-Curtis and PCD
335 dissimilarities followed by ANOSIM test evidenced a strong vertical mesozooplankton
336 structuring (according to depth) in both datasets (Figure 4E-H), which was consistently
337 observed in each oceanic region separately (Table 1). Horizontal structuring (according to
338 ocean basin) was clearly supported in *mICOI* dataset but was not (or weakly) supported in
339 *mac18S* (Figure 4A-D). Interestingly, mesozooplankton communities exhibited horizontal
340 structuring at epipelagic and mesopelagic layers (excepting in *mac18S*-PCD, where
341 mesozooplankton structuring was only observed at the epipelagic layer) but not at
342 bathypelagic depths by any combination of marker and beta-diversity parameter (Table 1).

343 Further, we found that bathypelagic communities were structured according to deep-water
344 mass type (as defined in Catalá et al. (2015)) rather than to oceanic basin.

345 *Horizontal and vertical patterns in mesozooplankton alpha- and beta-diversity*

346 We analysed how mesozooplankton alpha- and beta-diversity are globally structured along
347 the temperate to tropical global ocean. We did not observe consistent vertical nor
348 horizontal patterns in mesozooplankton alpha-diversity measurements among markers,
349 neither analysing the data globally (Figure S4A) nor by oceanic region (Figure S4B).

350 On the other hand, we observed a recurrent pattern of increasing beta-diversity between
351 mesozooplankton communities with depth (from the surface to the bathypelagic zone) in
352 both *mICOI* (Figure 5A) and *mac18S* datasets (Figure 6A), i.e., mesozooplankton
353 communities from the upper layers are more similar to each other than communities from
354 the lower mesopelagic and bathypelagic depths, indicating a greater connectivity between
355 mesozooplankton assemblages at the surface than at deeper ocean. This trend was evident
356 in *mICOI* dataset using Bray-Curtis distances and in *mac18S* using both Bray-Curtis and PCD
357 but less clear in *mICOI* using PCD. The pattern of increasing beta-diversity with depth turned
358 out more robust for each combination of marker and beta-diversity measurement when the
359 different oceanic regions were analysed separately (Figure 5B, 6B), and still quite apparent
360 when considering only the stations with all four depth ranges sampled (Figure S5).

361 *Relative contribution of environment and oceanic distance to mesozooplankton spatial* 362 *structuring*

363 To determine the factors driving mesozooplankton spatial distribution at each depth range,
364 we performed Mantel correlations between variations in mesozooplankton community
365 composition and variations in oceanic and environmental distances (Table 2, Figure S6).
366 Mesozooplankton community dissimilarities correlated significantly with oceanic distances
367 in both *m/COI* and *mac18S* datasets regardless of the beta-diversity measurement used
368 (except for 500-1000 m depth in *mac18S*), indicating the existence of distance-decay
369 patterns in mesozooplankton communities at all depth ranges. It was especially noticeable
370 at the upper oceanic layers, where oceanic distance was the main contributor to
371 mesozooplankton community composition. Less consistency was found regarding the
372 contribution of environmental distances to mesozooplankton spatial distribution among
373 markers—the environment noticeably determined mesozooplankton community
374 composition in *m/COI* but had limited influence in *mac18S* dataset—and among beta-
375 diversity measurements—with particularly different results in *mac18S* using Bray-Curtis and
376 PCD distances. In the bathypelagic layer, the relative contribution of the environment to
377 mesozooplankton community composition was overall higher than the oceanic distance,
378 yet not always statistically significant (Table 2). Among the parameters measured, oxygen,
379 temperature, conductivity, and salinity emerged as the ones most influencing
380 mesozooplankton communities. Oceanic and environmental distances were consistently
381 correlated at all depths, with remarkably high correlation values at bathypelagic depths
382 (Table 2).

383

384 **Discussion**

385 *Overview of mesozooplankton community composition across the tropical to temperate*
386 *global ocean*

387 Our findings identified Arthropoda—specifically Hexanauplia (copepods), and to a lesser
388 extent Ostracoda and Malacostraca (group including euphausiids and decapods)—as the
389 most abundant and diverse groups in the tropical to temperate global ocean, in agreement
390 with previous studies (Fernández de Puellas et al., 2019; La et al., 2015; Sommer et al., 2017;
391 Stefanoudis et al., 2019). Due to their high abundance and worldwide distribution, these
392 organisms are recognised as a central component of epipelagic marine ecosystems, playing
393 a key role as main link between lower (producers and primary consumers) and higher
394 trophic levels (Steinberg & Landry, 2017) and being the main food source of many
395 commercial fishes, thus sustaining a number of fisheries worldwide (Hays et al., 2005;
396 Turner, 2004). Our data suggest that marine arthropods are also dominant among
397 mesozooplankton at mesopelagic and bathypelagic depths, thus supporting a central role
398 of these organisms in the deep-ocean trophic web as well (Kelly et al., 2019), in addition to
399 their relevance modulating global biogeochemical processes such as the biological carbon
400 pump (Bode et al., 2018; Steinberg & Landry, 2017).

401 Although the taxonomic composition retrieved by both markers (*mICOI* and *mac18S*) was
402 very similar, some taxonomic groups were retrieved differently by one of the markers. This
403 fact highlights the importance of choosing an adequate barcode when designing
404 metabarcoding-based studies (Bucklin et al., 2016) and reinforces the need for multi-marker
405 approaches to get comprehensive insights on the zooplankton taxonomic diversity (Stefanni
406 et al., 2018; van der Loos & Nijland, 2021; G. K. Zhang, Chain, Abbott, & Cristescu, 2018). A

407 remarkable proportion of reads in both datasets at all depths under study were attributed
408 to gelatinous organisms (e.g., cnidarians or tunicates), which are normally underestimated
409 in morphologically based surveys using nets due to their fragility, and for which DNA-based
410 methods may be more effective (Bucklin et al., 2019; Govindarajan et al., 2021). Otherwise,
411 we acknowledge that we are probably missing some of the most abundant
412 mesozooplanktonic organisms in the ocean, such as *Oithona* spp. and other small-sized
413 Cyclopoids (Turner, 2004), most of which probably escaped our detection due to having a
414 body size smaller than the 300 μm mesh size used during the Malaspina sampling.
415 Additional studies including other size fractions could complement our findings by
416 confirming whether the global patterns observed here also apply for the smallest
417 mesozooplankton fraction.

418 *Focusing on the unknown – identifying hotspot areas of hidden diversity*

419 The presence of a high number of OTUs that could not be assigned to species level and that
420 were so distant to sequences from MZGdb (Bucklin et al., 2021), suggests that our
421 knowledge of the organisms inhabiting the pelagic open ocean it is still scarce, especially
422 beyond the epipelagic layer as also reported by other authors (Sommer et al., 2017), and
423 evidence that zooplankton molecular reference databases are far from completion (Bucklin
424 et al., 2010; Bucklin et al., 2021). According to our data, the Indian Ocean and the lower
425 mesopelagic and bathypelagic layers are the regions requiring further taxonomic and/or
426 sequencing efforts along the tropical to temperate latitudes. Our findings agree with Bucklin
427 et al. (2021), who placed the Indian Ocean among the oceanic basins with lower species
428 coverage by DNA barcoding initiatives (with only 29% of copepod species barcoded) and

429 considered the deep-sea ecosystems as an immediate priority for DNA barcoding and
430 metabarcoding studies. Additional initiatives to the ones from (Bucklin et al., 2010) and
431 other barcoding projects detailed therein are thus required in order to obtain these
432 references—while increasing our knowledge on zooplankton biodiversity—to ensure a
433 reliable application of DNA-based methods for the study of mesozooplankton.

434 *Mesozooplankton community composition exhibits vertical and horizontal biogeographic*
435 *patterns at a global scale*

436 Our results indicate that mesozooplankton community composition is structured across
437 both vertical and horizontal oceanic gradients. Vertical structuring was particularly strong
438 in both *mICOI* and *mac18S* datasets either analysing the data globally or at each oceanic
439 basin separately, thus adding evidence for a global, solid vertical structuring of
440 mesozooplankton in the ocean, corroborating many previous observations (Cheng et al.,
441 2022; Fernández de Puelles et al., 2019; Hirai et al., 2020; Pearman & Irigoien, 2015;
442 Sommer et al., 2017; Stefanoudis et al., 2019). Horizontal mesozooplankton structuring (i.e.,
443 according to oceanic basins) was also overall supported in both datasets, although it was
444 strongly supported in *mICOI* than in *mac18S*, most likely due to a higher capability of the
445 former to detect intraspecific genetic variants (Turon, Antich, Palacín, Præbel, &
446 Wangensteen, 2020), and thus better detect regional diversity and dissimilarities between
447 distant communities and populations (Chust et al., 2016).

448 Horizontal structuring of mesozooplankton communities has been widely reported at the
449 epipelagic layer and highlights the existence of biogeographic regions responding to

450 productivity, hydrology, environmental characteristics of water, and connectivity barriers
451 (Becker, Eiras Garcia, & Freire, 2018; de Vargas et al., 2015; Domínguez et al., 2017; Ershova,
452 Wangensteen, Descoteaux, Barth-Jensen, & Præbel, 2021; Feliú et al., 2020; Gaard et al.,
453 2008; Hirai & Tsuda, 2015), but few studies to date have assessed horizontal structuring of
454 mesozooplankton at meso- or bathypelagic depths (Hirai et al., 2020; Siokou et al., 2019).
455 Here, we observed that horizontal structuring of mesozooplankton community composition
456 along the temperate to tropical global ocean is unevenly supported across depth; it was
457 strongly supported at the epipelagic layer, moderately at mesopelagic depths, and low
458 supported in the bathypelagic zone. Although the latter finding was unexpected considering
459 the low connectivity of deep-sea mesozooplankton communities reported here—which
460 should lead to a more evident horizontal structuring, we observed that structuring of
461 mesozooplankton communities at bathypelagic depths was not determined by the oceanic
462 basin but by the deep-water mass type (as defined in Catalá et al. (2015)) from which they
463 were collected. Similar findings have been previously reported for prokaryotes (Agogué,
464 Lamy, Neal, Sogin, & Herndl, 2011; Salazar et al., 2016) and picoeukaryotes (Pernice et al.,
465 2016). Our results also indicate the existence of a distance-decay pattern (i.e., the farther
466 the communities the more different the community composition) for mesozooplankton
467 assemblages at all depths under study. Since this result may somehow indicate a
468 relationship between the oceanic distance and the deep-water mass type from which
469 bathypelagic samples were collected, further studies covering more samples and additional
470 deep-water mass types should be carried out in order to verify our findings.

471 *Vertical mesozooplankton alpha-diversity patterns are not ruled globally*

472 Previous studies on microzooplankton point to a general pattern of decreasing alpha-
473 diversity (richness and diversity indices) along the vertical oceanic gradient (Canals, Obiol,
474 Muhovic, Vaqué, & Massana, 2020; Countway et al., 2007; Giner et al., 2020); however, to
475 date there is no clear consensus on whether mesozooplankton alpha diversity increases or
476 decreases with depth. For instance, while a decreasing trend in mesozooplankton richness
477 and/or H index has been observed in Fernández de Puellas et al. (2019), Vereshchaka et al.
478 (2017), and Pearman and Irigoien (2015), among others, peaks in alpha-diversity at
479 mesopelagic or/and bathypelagic depths have also been reported for copepods (Hirai et al.,
480 2020; Kosobokova & Hirche, 2000; Stefanoudis et al., 2019) and for the whole
481 mesozooplankton community (Cheng et al., 2022; Sommer et al., 2017). Here, we did not
482 observe any consistent pattern in mesozooplankton alpha diversity with depth, but our
483 results seem to support the deep sea (down to the bathypelagic layer) as an ecosystem
484 harbouring a level of diversity comparable to the ones at upper depths. Based on the
485 discrepancies between the different studies, it is most likely that there is not a unique,
486 global pattern of mesozooplankton alpha diversity along the vertical profile in the ocean,
487 but that it is region specific. Further studies are thus needed to determine the factors
488 regulating mesozooplankton alpha diversity patterns along the vertical oceanic scale, such
489 as primary productivity and water column mixing.

490 In DNA-based studies, alpha diversity values in the deeper layers could be accounting for
491 the capture of mesozooplankton DNA sinking from upper layers (e.g., carcasses, attached
492 to sinking particles; Preston, Durkin, and Yamahara (2020)) and the stomach contents of
493 diel vertical migratory species, which move upward the water column to feed during the

494 night, returning to the depths at sun (Steinberg & Landry, 2017). Yet, this downward-
495 transported or prey material is expected to be less abundant and more degraded than the
496 one from the alive individuals comprising the samples, thus representing a neglecting
497 proportion of OTUs and reads. Also, it is interesting to note that DNA-based approaches are
498 known to yield higher diversity values (especially in richness) than morphologically based
499 surveys (Ershova et al., 2021; Schroeder et al., 2020; Sommer et al., 2017). In the deep
500 ocean, this bias between methods could be even magnified due to the notably lesser
501 knowledge on deep-sea mesozooplankton diversity—hampering its taxonomic
502 classification—and its overall lower abundance—making it less likely to be sampled.

503 *The deeper the lower the connectivity between mesozooplankton communities*

504 Results derived from the beta-diversity analyses indicated a higher dissimilarity between
505 mesozooplankton communities from the ocean deep layers (especially at the bathypelagic
506 zone) than between communities from the upper layers. These findings are in line with
507 those obtained by Siokou et al. (2019) in the Mediterranean Sea, who observed
508 differentiation between Eastern and Western Mediterranean mesozooplankton
509 communities at lower mesopelagic and bathypelagic depths, but no differentiation at
510 epipelagic and upper mesopelagic layers. These results point to lower connectivity between
511 deep-sea mesozooplankton communities than between communities from upper oceanic
512 layers, which may be driven by limitations in the dispersal of mesozooplankton assemblages
513 at the ocean depths due to prevailing weaker oceanic currents and water mixing in the deep
514 sea compared to the surface (Manral et al., 2023; Reid, 1981, 1994)—in agreement with
515 previous findings for picoeukaryotes (Villarino et al., 2022). Our findings add further

516 evidence on the major role of oceanic currents in shaping zooplankton dispersal and
517 connectivity at a global scale, not only at epipelagic layers as previously reported (Richter
518 et al., 2020; Villarino et al., 2018; Watson et al., 2011), but, for the first time for
519 mesozooplankton, also at the ocean depths. Yet, it should be noted that the relative
520 contribution of oceanic distance in shaping mesozooplankton communities at the ocean
521 depths was overall lower relative to the contribution of the environment. While oceanic
522 distance can be assumed as a proxy of oceanic currents at the epipelagic layer, this
523 assumption could lose strength deeper in the water column, since deep oceanic currents
524 may follow not only horizontal but also vertical and/or oblique routes due to the
525 thermohaline circulation.

526 *Contribution of dispersal and selection to mesozooplankton community composition in the*
527 *deep ocean*

528 The contribution of dispersal and environmental selection on plankton spatial distribution
529 has been reported to differ among groups and oceanic depths, as recently reported by
530 (Villarino et al., 2022). Here, our results suggested dispersal as the main contributor to
531 mesozooplankton distribution at the upper oceanic layers, attributing a secondary role to
532 environmental selection. At bathypelagic depths, selection was the main driver of
533 mesozooplankton community composition together with dispersal, even though the
534 bathypelagic zone is much more homogeneous in terms of environmental conditions than
535 the layers above it (Bode et al., 2018; Danovaro et al., 2004). Considering that dispersal of
536 plankton in the ocean is globally constrained by environmental selection (Ward, Cael,
537 Collins, & Young, 2021), our results indicate that little environmental variations in the

538 bathypelagic layer may generate more marked differences in mesozooplankton beta-
539 diversity than at upper depths. Yet evaluating the specific contribution of environmental
540 and oceanic distances (i.e., selection and dispersal, respectively) in the present study is
541 challenging due to the significant, consistent correlation between both factors, specially at
542 the bathypelagic layer. Between 1000 and 3000 m depth, environmental and oceanic
543 distances appeared to be markedly correlated, thus somehow blurring the boundary
544 between dispersal and environmental selection when aiming to interpret the results. As
545 observed in the present study and in previous works (Agogué et al., 2011; Pernice et al.,
546 2016; Salazar et al., 2016), plankton community composition in the deep ocean appears to
547 be highly related to the deep-water mass type at which they are found, which are in turn
548 defined according to its environmental characteristics (Catalá et al., 2015) and present
549 limited mixing with the surrounding water masses (Reid, 1981). Thus, although our findings
550 clearly support that mesozooplankton communities show biogeographic patterns in the
551 deep ocean, to elucidate whether these patterns are primarily driven by dispersal or by
552 environmental selection will require further research including the collection of more
553 samples from additional deep-water mass types.

554 Despite the main role of dispersal in shaping mesozooplankton community composition,
555 correlation between environmental variables and mesozooplankton community
556 composition was also found at all depth ranges under study, which supports the view that
557 global structuring of planktonic communities is vulnerable to climate change-derived effects
558 (Benedetti et al., 2021; Villarino et al., 2015), particularly at the ocean depths, where
559 environmental conditions are more stable (Bode et al., 2018; Danovaro et al., 2004). The

560 consequences derived from alterations in global mesozooplankton structuring on the whole
561 marine ecosystem services are still uncertain, but they are expected to be significant
562 considering the central role of mesozooplankton in the oceanic tropic web and in
563 biogeochemical processes (Danovaro, Corinaldesi, Dell'Anno, & Snelgrove, 2017; Kelly et
564 al., 2019; Steinberg & Landry, 2017).

565

566 **Acknowledgements**

567 The samples analysed in this study were collected during the Malaspina Circumnavigation
568 Expedition, funded by the Spanish Ministry of Economy and Competitiveness (Consolider-
569 Ingenio 2010, CSD2008-00077, CTM 2012-39587-C04 and CTM2016-78853-R). This research
570 has been funded by the Department of Agriculture and Fisheries of the Basque government
571 (project GENGES) and by the European Union's Horizon 2020 research and innovation
572 programme under Grant Agreement No 862428 (project MISSION ATLANTIC). Eva Aylagas
573 and Jon Corell were supported by the Fundación Centros Tecnológicos through an Iñaki
574 Goenaga doctoral grant. We thank the participants of the Malaspina Expedition and the
575 crew of the R.V. Hespérides for their assistance during the 7-month cruise and specially
576 Maite Cuesta Trula for assistance with the mesozooplankton samples. This paper is
577 contribution nº xxxx from AZTI, Marine Research, Basque Research and Technology Alliance
578 (BRTA).

579

580

581 **References**

- 582 Agogu , H., Lamy, D., Neal, P. R., Sogin, M. L., & Herndl, G. J. (2011). Water mass-specificity of
583 bacterial communities in the North Atlantic revealed by massively parallel sequencing.
584 *Molecular Ecology*, *20*(2), 258-274. doi:<https://doi.org/10.1111/j.1365-294X.2010.04932.x>
- 585 Altschul, S. F., Gish, W., Miller, W., Myers, E. W., & Lipman, D. J. (1990). Basic local alignment
586 search tool. *J Mol Biol*, *215*(3), 403-410. doi:10.1016/s0022-2836(05)80360-2
- 587 Becker,  . C., Eiras Garcia, C. A., & Freire, A. S. (2018). Mesozooplankton distribution, especially
588 copepods, according to water masses dynamics in the upper layer of the Southwestern
589 Atlantic shelf (26 S to 29 S). *Continental Shelf Research*, *166*, 10-21.
590 doi:<https://doi.org/10.1016/j.csr.2018.06.011>
- 591 Benedetti, F., Vogt, M., Elizondo, U. H., Righetti, D., Zimmermann, N. E., & Gruber, N. (2021).
592 Major restructuring of marine plankton assemblages under global warming. *Nature*
593 *Communications*, *12*(1), 5226. doi:10.1038/s41467-021-25385-x
- 594 Bode, M., Koppelman, R., Teuber, L., Hagen, W., & Auel, H. (2018). Carbon Budgets of
595 Mesozooplankton Copepod Communities in the Eastern Atlantic Ocean—Regional and
596 Vertical Patterns Between 24 N and 21 S. *Global Biogeochemical Cycles*, *32*(5), 840-857.
597 doi:<https://doi.org/10.1029/2017GB005807>
- 598 Bolger, A. M., Lohse, M., & Usadel, B. (2014). Trimmomatic: a flexible trimmer for Illumina
599 sequence data. *Bioinformatics*, *30*(15), 2114-2120. doi:10.1093/bioinformatics/btu170
- 600 Brand o, M. C., Benedetti, F., Martini, S., Soviadan, Y. D., Irisson, J.-O., Romagnan, J.-B., . . . Tara
601 Oceans Consortium, C. (2021). Macroscale patterns of oceanic zooplankton composition
602 and size structure. *Scientific Reports*, *11*(1), 15714. doi:10.1038/s41598-021-94615-5
- 603 Bucklin, A., Lindeque, P. K., Rodriguez-Ezpeleta, N., Albaina, A., & Lehtiniemi, M. (2016).
604 Metabarcoding of marine zooplankton: prospects, progress and pitfalls. *Journal of*
605 *Plankton Research*, *38*(3), 393-400. doi:10.1093/plankt/fbw023
- 606 Bucklin, A., Ortman, B. D., Jennings, R. M., Nigro, L. M., Sweetman, C. J., Copley, N. J., . . . Wiebe, P.
607 H. (2010). A “Rosetta Stone” for metazoan zooplankton: DNA barcode analysis of species
608 diversity of the Sargasso Sea (Northwest Atlantic Ocean). *Deep Sea Research Part II:*
609 *Topical Studies in Oceanography*, *57*(24), 2234-2247.
610 doi:<https://doi.org/10.1016/j.dsr2.2010.09.025>
- 611 Bucklin, A., Peijnenburg, K. T. C. A., Kosobokova, K. N., O’Brien, T. D., Blanco-Bercial, L., Cornils, A.,
612 . . . Weydmann-Zwolicka, A. (2021). Toward a global reference database of COI barcodes
613 for marine zooplankton. *Marine Biology*, *168*(6), 78. doi:10.1007/s00227-021-03887-y
- 614 Bucklin, A., Yeh, H. D., Questel, J. M., Richardson, D. E., Reese, B., Copley, N. J., & Wiebe, P. H.
615 (2019). Time-series metabarcoding analysis of zooplankton diversity of the NW Atlantic
616 continental shelf. *ICES Journal of Marine Science*, *76*(4), 1162-1176.
617 doi:10.1093/icesjms/fsz021
- 618 Calbet, A. (2001). Mesozooplankton grazing effect on primary production: A global comparative
619 analysis in marine ecosystems. *Limnology and Oceanography*, *46*(7), 1824-1830.
620 doi:<https://doi.org/10.4319/lo.2001.46.7.1824>
- 621 Canals, O., Obiol, A., Muhovic, I., Vaqu , D., & Massana, R. (2020). Ciliate diversity and distribution
622 across horizontal and vertical scales in the open ocean. *Molecular Ecology*, *29*(15), 2824-
623 2839. doi:<https://doi.org/10.1111/mec.15528>
- 624 Carlotti, F., Pagano, M., Guilloux, L., Donoso, K., Vald s, V., Grosso, O., & Hunt, B. (2018). Meso-
625 zooplankton structure and functioning in the western tropical South Pacific along the 20th

626 parallel south during the OUTPACE survey (February April 2015). *Biogeosciences*, 15, 7273-
627 7297.

628 Casteleyn, G., Leliaert, F., Backeljau, T., Debeer, A.-E., Kotaki, Y., Rhodes, L., . . . Vyverman, W.
629 (2010). Limits to gene flow in a cosmopolitan marine planktonic diatom. *Proceedings of*
630 *the National Academy of Sciences*, 107(29), 12952-12957. doi:10.1073/pnas.1001380107

631 Catalá, T. S., Reche, I., Fuentes-Lema, A., Romera-Castillo, C., Nieto-Cid, M., Ortega-Retuerta, E., . .
632 . Álvarez-Salgado, X. A. (2015). Turnover time of fluorescent dissolved organic matter in
633 the dark global ocean. *Nature Communications*, 6(1), 5986. doi:10.1038/ncomms6986

634 Cermeño, P., de Vargas, C., Abrantes, F., & Falkowski, P. G. (2010). Phytoplankton Biogeography
635 and Community Stability in the Ocean. *PLOS ONE*, 5(4), e10037.
636 doi:10.1371/journal.pone.0010037

637 Cheng, X.-W., Zhang, L.-L., Gao, F., Tan, Y.-H., Xiang, R., Qiu, Z.-Y., & He, L.-J. (2022). Biodiversity of
638 zooplankton in 0–3000 m waters from the eastern Indian Ocean in spring 2019 based on
639 metabarcoding. *Water Biology and Security*, 1(1), 100005.
640 doi:<https://doi.org/10.1016/j.watbs.2022.100005>

641 Chiba, S., Batten, S., Martin, C. S., Ivory, S., Miloslavich, P., & Weatherdon, L. V. (2018).
642 Zooplankton monitoring to contribute towards addressing global biodiversity conservation
643 challenges. *Journal of Plankton Research*, 40(5), 509-518. doi:10.1093/plankt/fby030

644 Chust, G., Irigoien, X., Chave, J., & Harris, R. P. (2013). Latitudinal phytoplankton distribution and
645 the neutral theory of biodiversity. *Global Ecology and Biogeography*, 22(5), 531-543.
646 doi:<https://doi.org/10.1111/geb.12016>

647 Chust, G., Villarino, E., Chenuil, A., Irigoien, X., Bizsel, N., Bode, A., . . . Borja, A. (2016). Dispersal
648 similarly shapes both population genetics and community patterns in the marine realm.
649 *Scientific Reports*, 6(1), 28730. doi:10.1038/srep28730

650 Chust, G., Vogt, M., Benedetti, F., Nakov, T., Villéger, S., Aubert, A., . . . Ayata, S.-D. (2017). Mare
651 Incognitum: A Glimpse into Future Plankton Diversity and Ecology Research. *Frontiers in*
652 *Marine Science*, 4.

653 Clarke, K. R. (1993). Non-parametric multivariate analyses of changes in community structure.
654 *Australian Journal of Ecology*, 18(1), 117-143. doi:[https://doi.org/10.1111/j.1442-
655 9993.1993.tb00438.x](https://doi.org/10.1111/j.1442-9993.1993.tb00438.x)

656 Countway, P. D., Gast, R. J., Dennett, M. R., Savai, P., Rose, J. M., & Caron, D. A. (2007). Distinct
657 protistan assemblages characterize the euphotic zone and deep sea (2500 m) of the
658 western North Atlantic (Sargasso Sea and Gulf Stream). *Environmental Microbiology*, 9(5),
659 1219-1232. doi:<https://doi.org/10.1111/j.1462-2920.2007.01243.x>

660 Danovaro, R., Corinaldesi, C., Dell'Anno, A., & Snelgrove, P. V. R. (2017). The deep-sea under global
661 change. *Current Biology*, 27(11), R461-R465.
662 doi:<https://doi.org/10.1016/j.cub.2017.02.046>

663 Danovaro, R., Dell'Anno, A., & Pusceddu, A. (2004). Biodiversity response to climate change in a
664 warm deep sea. *Ecology Letters*, 7(9), 821-828. doi:[https://doi.org/10.1111/j.1461-
665 0248.2004.00634.x](https://doi.org/10.1111/j.1461-0248.2004.00634.x)

666 de Vargas, C., Audic, S., Henry, N., Decelle, J., Mahé, F., Logares, R., . . . Velayoudon, D. (2015).
667 Eukaryotic plankton diversity in the sunlit ocean. *Science*, 348(6237), 1261605.
668 doi:10.1126/science.1261605

669 Domínguez, R., Garrido, S., Santos, A. M. P., & dos Santos, A. (2017). Spatial patterns of
670 mesozooplankton communities in the Northwestern Iberian shelf during autumn shaped
671 by key environmental factors. *Estuarine, Coastal and Shelf Science*, 198, 257-268.
672 doi:<https://doi.org/10.1016/j.ecss.2017.09.008>

673 Dornelas, M., Connolly, S. R., & Hughes, T. P. (2006). Coral reef diversity refutes the neutral theory
674 of biodiversity. *Nature*, 440(7080), 80-82. doi:10.1038/nature04534

675 Duarte, C. M. (2015). Seafaring in the 21st Century: The Malaspina 2010 Circumnavigation
676 Expedition. *Limnology and Oceanography Bulletin*, 24(1), 11-14.
677 doi:<https://doi.org/10.1002/lob.10008>

678 Ducklow, H. W., Steinberg, D. K., & Buesseler, K. O. (2001). Upper Ocean Carbon Export and the
679 Biological Pump. *Oceanography*, 14(4), 50-58.
680 doi:<https://doi.org/10.5670/oceanog.2001.06>

681 Edgar, R. C., Haas, B. J., Clemente, J. C., Quince, C., & Knight, R. (2011). UCHIME improves
682 sensitivity and speed of chimera detection. *Bioinformatics*, 27(16), 2194-2200.
683 doi:10.1093/bioinformatics/btr381

684 Ershova, E. A., & Kosobokova, K. N. (2019). Cross-shelf structure and distribution of
685 mesozooplankton communities in the East-Siberian Sea and the adjacent Arctic Ocean.
686 *Polar Biology*, 42(7), 1353-1367. doi:10.1007/s00300-019-02523-2

687 Ershova, E. A., Wangenstein, O. S., Descoteaux, R., Barth-Jensen, C., & Præbel, K. (2021).
688 Metabarcoding as a quantitative tool for estimating biodiversity and relative biomass of
689 marine zooplankton. *ICES Journal of Marine Science*, 78(9), 3342-3355.
690 doi:10.1093/icesjms/fsab171

691 Feliú, G., Pagano, M., Hidalgo, P., & Carlotti, F. (2020). Structure and function of epipelagic
692 mesozooplankton and their response to dust deposition events during the spring
693 PEACETIME cruise in the Mediterranean Sea. *Biogeosciences*, 17(21), 5417-5441.
694 doi:10.5194/bg-17-5417-2020

695 Fernández de Puelles, M. L., Gazá, M., Cabanellas-Reboredo, M., Santandreu, M. D., Irigoien, X.,
696 González-Gordillo, J. I., . . . Hernández-León, S. (2019). Zooplankton Abundance and
697 Diversity in the Tropical and Subtropical Ocean. *Diversity*, 11(11). doi:10.3390/d11110203

698 Fiksen, Ø., Jørgensen, C., Kristiansen, T., Vikebø, F., & Huse, G. (2007). Linking behavioural ecology
699 and oceanography: Larval behaviour determines growth, mortality and dispersal. *Marine
700 Ecology Progress Series*, 347, 195-205. doi:10.3354/meps06978

701 Gaard, E., Gislason, A., Falkenhaug, T., Sjøiland, H., Musaeva, E., Vereshchaka, A., & Vinogradov, G.
702 (2008). Horizontal and vertical copepod distribution and abundance on the Mid-Atlantic
703 Ridge in June 2004. *Deep Sea Research Part II: Topical Studies in Oceanography*, 55(1), 59-
704 71. doi:<https://doi.org/10.1016/j.dsr2.2007.09.012>

705 Gilbert, B., & Levine, J. M. (2017). Ecological drift and the distribution of species diversity.
706 *Proceedings of the Royal Society B: Biological Sciences*, 284(1855), 20170507.
707 doi:10.1098/rspb.2017.0507

708 Giner, C. R., Pernice, M. C., Balagué, V., Duarte, C. M., Gasol, J. M., Logares, R., & Massana, R.
709 (2020). Marked changes in diversity and relative activity of picoeukaryotes with depth in
710 the world ocean. *The ISME Journal*, 14(2), 437-449. doi:10.1038/s41396-019-0506-9

711 Govindarajan, A. F., Francolini, R. D., Jech, J. M., Lavery, A. C., Llopiz, J. K., Wiebe, P. H., & Zhang,
712 W. (2021). Exploring the Use of Environmental DNA (eDNA) to Detect Animal Taxa in the
713 Mesopelagic Zone. *Frontiers in Ecology and Evolution*, 9. doi:10.3389/fevo.2021.574877

714 Guidi, L., Chaffron, S., Bittner, L., Eveillard, D., Larhlimi, A., Roux, S., . . . Tara Oceans Consortium, C.
715 (2016). Plankton networks driving carbon export in the oligotrophic ocean. *Nature*,
716 532(7600), 465-470. doi:10.1038/nature16942

717 Hays, G. C., Richardson, A. J., & Robinson, C. (2005). Climate change and marine plankton. *Trends
718 in Ecology & Evolution*, 20(6), 337-344. doi:<https://doi.org/10.1016/j.tree.2005.03.004>

719 Hellweger, F. L., van Sebille, E., & Fredrick, N. D. (2014). Biogeographic patterns in ocean microbes
720 emerge in a neutral agent-based model. *Science*, *345*(6202), 1346-1349.
721 doi:10.1126/science.1254421

722 Hernández-León, S., Koppelman, R., Fraile-Nuez, E., Bode, A., Mompeán, C., Irigoien, X., . . .
723 Duarte, C. M. (2020). Large deep-sea zooplankton biomass mirrors primary production in
724 the global ocean. *Nature Communications*, *11*(1), 6048. doi:10.1038/s41467-020-19875-7

725 Hirai, Tachibana, A., & Tsuda, A. (2020). Large-scale metabarcoding analysis of epipelagic and
726 mesopelagic copepods in the Pacific. *PLOS ONE*, *15*(5), e0233189.
727 doi:10.1371/journal.pone.0233189

728 Hirai, & Tsuda, A. (2015). Metagenetic community analysis of epipelagic planktonic copepods in
729 the tropical and subtropical Pacific. *Marine Ecology Progress Series*, *534*, 65-78.

730 Hubbell, S. P. (2001). *The Unified Neutral Theory of Biodiversity and Biogeography (MPB-32)*:
731 Princeton University Press.

732 Hutchinson, G. E. (1957). Concluding Remarks. *Cold Spring Harbor Symposia on Quantitative
733 Biology*, *22*, 415-427.

734 Ibarbalz, F. M., Henry, N., Brandão, M. C., Martini, S., Busseni, G., Byrne, H., . . . Zinger, L. (2019).
735 Global Trends in Marine Plankton Diversity across Kingdoms of Life. *Cell*, *179*(5), 1084-
736 1097.e1021. doi:<https://doi.org/10.1016/j.cell.2019.10.008>

737 Jeraldo, P., Kalari, K., Chen, X., Bhavsar, J., Mangalam, A., White, B., . . . Chia, N. (2014). IM-
738 TORNADO: A Tool for Comparison of 16S Reads from Paired-End Libraries. *PLOS ONE*,
739 *9*(12), e114804. doi:10.1371/journal.pone.0114804

740 Kelly, T. B., Davison, P. C., Goericke, R., Landry, M. R., Ohman, M. D., & Stukel, M. R. (2019). The
741 Importance of Mesozooplankton Diel Vertical Migration for Sustaining a Mesopelagic Food
742 Web. *Frontiers in Marine Science*, *6*. doi:10.3389/fmars.2019.00508

743 Kembel, S. W., Cowan, P. D., Helmus, M. R., Cornwell, W. K., Morlon, H., Ackerly, D. D., . . . Webb,
744 C. O. (2010). Picante: R tools for integrating phylogenies and ecology. *Bioinformatics*,
745 *26*(11), 1463-1464. doi:10.1093/bioinformatics/btq166

746 Kim, H., Lee, C.-R., Lee, S.-k., Oh, S.-Y., & Kim, W. (2020). Biodiversity and Community Structure of
747 Mesozooplankton in the Marine and Coastal National Park Areas of Korea. *Diversity*, *12*(6).
748 doi:10.3390/d12060233

749 Kosobokova, K., & Hirche, H. J. (2000). Zooplankton distribution across the Lomonosov Ridge,
750 Arctic Ocean: species inventory, biomass and vertical structure. *Deep Sea Research Part I:
751 Oceanographic Research Papers*, *47*(11), 2029-2060. doi:[https://doi.org/10.1016/S0967-
752 0637\(00\)00015-7](https://doi.org/10.1016/S0967-0637(00)00015-7)

753 La, H. S., Kang, M., Dahms, H.-U., Ha, H. K., Yang, E. J., Lee, H., . . . Kang, S.-H. (2015).
754 Characteristics of mesozooplankton sound-scattering layer in the Pacific Summer Water,
755 Arctic Ocean. *Deep Sea Research Part II: Topical Studies in Oceanography*, *120*, 114-123.
756 doi:<https://doi.org/10.1016/j.dsr2.2015.01.005>

757 Landry, M. R., Hood, R. R., & Davies, C. H. (2020). Mesozooplankton biomass and temperature-
758 enhanced grazing along a 110°E transect in the eastern Indian Ocean. *Marine Ecology
759 Progress Series*, *649*, 1-19.

760 Leray, M., Yang, J. Y., Meyer, C. P., Mills, S. C., Agudelo, N., Ranwez, V., . . . Machida, R. J. (2013). A
761 new versatile primer set targeting a short fragment of the mitochondrial COI region for
762 metabarcoding metazoan diversity: application for characterizing coral reef fish gut
763 contents. *Frontiers in Zoology*, *10*(1), 34. doi:10.1186/1742-9994-10-34

764 Lindeque, P. K., Parry, H. E., Harmer, R. A., Somerfield, P. J., & Atkinson, A. (2013). Next Generation
765 Sequencing Reveals the Hidden Diversity of Zooplankton Assemblages. *PLOS ONE*, *8*(11),
766 e81327. doi:10.1371/journal.pone.0081327

767 Liszka, C. M., Manno, C., Stowasser, G., Robinson, C., & Tarling, G. A. (2019). Mesozooplankton
768 Community Composition Controls Fecal Pellet Flux and Remineralization Depth in the
769 Southern Ocean. *Frontiers in Marine Science*, 6(230). doi:10.3389/fmars.2019.00230

770 Machida, R. J., & Knowlton, N. (2012). PCR Primers for Metazoan Nuclear 18S and 28S Ribosomal
771 DNA Sequences. *PLOS ONE*, 7(9), e46180. doi:10.1371/journal.pone.0046180

772 Magoč, T., & Salzberg, S. L. (2011). FLASH: fast length adjustment of short reads to improve
773 genome assemblies. *Bioinformatics*, 27(21), 2957-2963.
774 doi:10.1093/bioinformatics/btr507

775 Mahé, F., Rognes, T., Quince, C., de Vargas, C., & Dunthorn, M. (2014). Swarm: robust and fast
776 clustering method for amplicon-based studies. *PeerJ*, 2, e593-e593. doi:10.7717/peerj.593

777 Manral, D., Iovino, D., Jaillon, O., Masina, S., Sarmiento, H., Ludicone, D., . . . van Sebille, E. (2023).
778 Computing marine plankton connectivity under thermal constraints. *Frontiers in Marine
779 Science*, 10.

780 Nekola, J. C., & White, P. S. (1999). The distance decay of similarity in biogeography and ecology.
781 *Journal of Biogeography*, 26(4), 867-878. doi:[https://doi.org/10.1046/j.1365-
782 2699.1999.00305.x](https://doi.org/10.1046/j.1365-2699.1999.00305.x)

783 Ohman, M. D. (1990). The Demographic Benefits of Diel Vertical Migration by Zooplankton.
784 *Ecological Monographs*, 60(3), 257-281. doi:10.2307/1943058

785 Oksanen, J., Blanchet, F. G., Friendly, M., Kindt, R., Legendre, P., McGlenn, D., & Wagner, H. (2019).
786 vegan: Community Ecology Package., <https://CRAN.R-project.org/package=vegan>.

787 Pante, E., & Simon-Bouhet, B. (2013). marmap: A Package for Importing, Plotting and Analyzing
788 Bathymetric and Topographic Data in R. *PLOS ONE*, 8(9), e73051.
789 doi:10.1371/journal.pone.0073051

790 Pearman, J. K., & Irigoien, X. (2015). Assessment of Zooplankton Community Composition along a
791 Depth Profile in the Central Red Sea. *PLOS ONE*, 10(7), e0133487.
792 doi:10.1371/journal.pone.0133487

793 Pernice, M. C., Giner, C. R., Logares, R., Perera-Bel, J., Acinas, S. G., Duarte, C. M., . . . Massana, R.
794 (2016). Large variability of bathypelagic microbial eukaryotic communities across the
795 world's oceans. *The ISME Journal*, 10(4), 945-958. doi:10.1038/ismej.2015.170

796 Preston, C. M., Durkin, C. A., & Yamahara, K. M. (2020). DNA metabarcoding reveals organisms
797 contributing to particulate matter flux to abyssal depths in the North East Pacific ocean.
798 *Deep Sea Research Part II: Topical Studies in Oceanography*, 173, 104708.
799 doi:<https://doi.org/10.1016/j.dsr2.2019.104708>

800 Pueyo, S. (2006). Diversity: between neutrality and structure. *Oikos*, 112(2), 392-405.
801 doi:<https://doi.org/10.1111/j.0030-1299.2006.14188.x>

802 Quast, C., Pruesse, E., Yilmaz, P., Gerken, J., Schweer, T., Yarza, P., . . . Glöckner, F. O. (2013). The
803 SILVA ribosomal RNA gene database project: improved data processing and web-based
804 tools. *Nucleic Acids Research*, 41(D1), D590-D596. doi:10.1093/nar/gks1219

805 R Core Development Team. (2013). R: A language and environment for statistical computing. . R
806 Foundation for Statistical Computing, Vienna, Austria. ISBN 3-900051-07-0. [http://www.R-
807 project.org/](http://www.R-project.org/).

808 Ratnarajah, L., Abu-Alhaija, R., Atkinson, A., Batten, S., Bax, N. J., Bernard, K. S., . . . Yebra, L.
809 (2023). Monitoring and modelling marine zooplankton in a changing climate. *Nature
810 Communications*, 14(1), 564. doi:10.1038/s41467-023-36241-5

811 Reid, J. L. (1969). Preliminary Results of Measurements of Deep Currents in the Pacific Ocean.
812 *Nature*, 221(5183), 848-848. doi:10.1038/221848a0

813 Reid, J. L. (1981). On the mid-depth circulation of the world ocean. *Evolution of Physical
814 Oceanography*, 623, 70-111.

815 Reid, J. L. (1994). On the total geostrophic circulation of the North Atlantic Ocean: Flow patterns,
816 tracers, and transports. *Progress in Oceanography*, 33(1), 1-92.
817 doi:[https://doi.org/10.1016/0079-6611\(94\)90014-0](https://doi.org/10.1016/0079-6611(94)90014-0)

818 Richter, D. J., Watteaux, R., Vannier, T., Leconte, J., Frémont, P., Reygondeau, G., . . . Jaillon, O.
819 (2020). Genomic evidence for global ocean plankton biogeography shaped by large-scale
820 current systems. *bioRxiv*, 867739. doi:10.1101/867739

821 Salazar, G., Cornejo-Castillo, F. M., Benítez-Barrios, V., Fraile-Nuez, E., Álvarez-Salgado, X. A.,
822 Duarte, C. M., . . . Acinas, S. G. (2016). Global diversity and biogeography of deep-sea
823 pelagic prokaryotes. *The ISME Journal*, 10(3), 596-608. doi:10.1038/ismej.2015.137

824 Saporiti, F., Bearhop, S., Vales, D. G., Silva, L., Zenteno, L., Tavares, M., . . . Cardona, L. (2015).
825 Latitudinal changes in the structure of marine food webs in the Southwestern Atlantic
826 Ocean. *Marine Ecology Progress Series*, 538, 23-34.

827 Schloss, P. D., Westcott, S. L., Ryabin, T., Hall, J. R., Hartmann, M., Hollister, E. B., . . . Weber, C. F.
828 (2009). Introducing mothur: Open-Source, Platform-Independent, Community-Supported
829 Software for Describing and Comparing Microbial Communities. *Applied and
830 Environmental Microbiology*, 75(23), 7537-7541. doi:10.1128/AEM.01541-09

831 Schroeder, A., Stanković, D., Pallavicini, A., Gionchetti, F., Pansera, M., & Camatti, E. (2020). DNA
832 metabarcoding and morphological analysis - Assessment of zooplankton biodiversity in
833 transitional waters. *Marine Environmental Research*, 160, 104946.
834 doi:<https://doi.org/10.1016/j.marenvres.2020.104946>

835 Siokou, I., Zervoudaki, S., Velaoras, D., Theocharis, A., Christou, E. D., Protopapa, M., & Pantazi, M.
836 (2019). Mesozooplankton vertical patterns along an east-west transect in the oligotrophic
837 Mediterranean sea during early summer. *Deep Sea Research Part II: Topical Studies in
838 Oceanography*, 164, 170-189. doi:<https://doi.org/10.1016/j.dsr2.2019.02.006>

839 Soininen, J., Lennon, J. J., & Hillebrand, H. (2007). A MULTIVARIATE ANALYSIS OF BETA DIVERSITY
840 ACROSS ORGANISMS AND ENVIRONMENTS. *Ecology*, 88(11), 2830-2838.
841 doi:<https://doi.org/10.1890/06-1730.1>

842 Sommer, S. A., Van Woudenberg, L., Lenz, P. H., Cepeda, G., & Goetze, E. (2017). Vertical gradients
843 in species richness and community composition across the twilight zone in the North
844 Pacific Subtropical Gyre. *Molecular Ecology*, 26(21), 6136-6156.
845 doi:<https://doi.org/10.1111/mec.14286>

846 Soviadan, Y. D., Benedetti, F., Brandão, M. C., Ayata, S.-D., Irissou, J.-O., Jamet, J. L., . . . Stemmann,
847 L. (2022). Patterns of mesozooplankton community composition and vertical fluxes in the
848 global ocean. *Progress in Oceanography*, 200, 102717.
849 doi:<https://doi.org/10.1016/j.pocean.2021.102717>

850 St. John, M. A., Borja, A., Chust, G., Heath, M., Grigorov, I., Mariani, P., . . . Santos, R. S. (2016). A
851 Dark Hole in Our Understanding of Marine Ecosystems and Their Services: Perspectives
852 from the Mesopelagic Community. *Frontiers in Marine Science*, 3.
853 doi:10.3389/fmars.2016.00031

854 Stefanni, S., Stanković, D., Borme, D., de Olazabal, A., Juretić, T., Pallavicini, A., & Tirelli, V. (2018).
855 Multi-marker metabarcoding approach to study mesozooplankton at basin scale. *Scientific
856 Reports*, 8(1), 12085. doi:10.1038/s41598-018-30157-7

857 Stefanoudis, P. V., Rivers, M., Ford, H., Yashayaev, I. M., Rogers, A. D., & Woodall, L. C. (2019).
858 Changes in zooplankton communities from epipelagic to lower mesopelagic waters.
859 *Marine Environmental Research*, 146, 1-11.
860 doi:<https://doi.org/10.1016/j.marenvres.2019.02.014>

861 Steinberg, D. K., & Landry, M. R. (2017). Zooplankton and the Ocean Carbon Cycle. *Annual Review
862 of Marine Science*, 9(1), 413-444. doi:10.1146/annurev-marine-010814-015924

863 Turner, J. T. (2004). The Importance of Small Planktonic Copepods and Their Roles in Pelagic
864 Marine Food Webs. *Zoological Studies*, 43, 255-266.

865 Turon, X., Antich, A., Palacín, C., Præbel, K., & Wangensteen, O. S. (2020). From metabarcoding to
866 metaphylogeography: separating the wheat from the chaff. *Ecological Applications*, 30(2),
867 e02036. doi:<https://doi.org/10.1002/eap.2036>

868 van der Loos, L. M., & Nijland, R. (2021). Biases in bulk: DNA metabarcoding of marine
869 communities and the methodology involved. *Molecular Ecology*, 30(13), 3270-3288.
870 doi:<https://doi.org/10.1111/mec.15592>

871 Vellend, M. (2010). Conceptual synthesis in community ecology. *The Quarterly review of biology*,
872 85(2), 183-206. doi:<https://doi.org/10.1086/652373>

873 Vereshchaka, A., Abyzova, G., Lunina, A., & Musaeva, E. (2017). The deep-sea zooplankton of the
874 North, Central, and South Atlantic: Biomass, abundance, diversity. *Deep Sea Research Part*
875 *II: Topical Studies in Oceanography*, 137, 89-101.
876 doi:<https://doi.org/10.1016/j.dsr2.2016.06.017>

877 Villarino, E., Chust, G., Licandro, P., Butenschön, M., Ibaibarriaga, L., Larrañaga, A., & Irigoien, X.
878 (2015). Modelling the future biogeography of North Atlantic zooplankton communities in
879 response to climate change. *Marine Ecology Progress Series*, 531, 121-142.

880 Villarino, E., Watson, J. R., Chust, G., Woodill, A. J., Klempay, B., Jonsson, B., . . . Barton, A. D.
881 (2022). Global beta diversity patterns of microbial communities in the surface and deep
882 ocean. *Global Ecology and Biogeography*, n/a(n/a). doi:<https://doi.org/10.1111/geb.13572>

883 Villarino, E., Watson, J. R., Jönsson, B., Gasol, J. M., Salazar, G., Acinas, S. G., . . . Chust, G. (2018).
884 Large-scale ocean connectivity and planktonic body size. *Nature Communications*, 9(1),
885 142. doi:10.1038/s41467-017-02535-8

886 Wang, Q., Garrity, G. M., Tiedje, J. M., & Cole, J. R. (2007). Naïve Bayesian Classifier for Rapid
887 Assignment of rRNA Sequences into the New Bacterial Taxonomy. *Applied and*
888 *Environmental Microbiology*, 73(16), 5261-5267. doi:10.1128/AEM.00062-07

889 Ward, B. A., Cael, B. B., Collins, S., & Young, C. R. (2021). Selective constraints on global plankton
890 dispersal. *Proceedings of the National Academy of Sciences*, 118(10), e2007388118.
891 doi:10.1073/pnas.2007388118

892 Watson, J. R., Hays, C. G., Raimondi, P. T., Mitarai, S., Dong, C., McWilliams, J. C., . . . Siegel, D. A.
893 (2011). Currents connecting communities: nearshore community similarity and ocean
894 circulation. *Ecology*, 92(6), 1193-1200. doi:<https://doi.org/10.1890/10-1436.1>

895 Whittaker, R. H. (1960). Vegetation of the Siskiyou Mountains, Oregon and California. *Ecological*
896 *Monographs*, 30(3), 279-338. doi:<https://doi.org/10.2307/1943563>

897 Zeldis, J. R., & Décima, M. (2020). Mesozooplankton connect the microbial food web to higher
898 trophic levels and vertical export in the New Zealand Subtropical Convergence Zone. *Deep*
899 *Sea Research Part I: Oceanographic Research Papers*, 155, 103146.
900 doi:<https://doi.org/10.1016/j.dsr.2019.103146>

901 Zhang, G. K., Chain, F. J. J., Abbott, C. L., & Cristescu, M. E. (2018). Metabarcoding using
902 multiplexed markers increases species detection in complex zooplankton communities.
903 *Evolutionary Applications*, 11(10), 1901-1914. doi:<https://doi.org/10.1111/eva.12694>

904 Zhang, X., & Dam, H. G. (1997). Downward export of carbon by diel migrant mesozooplankton in
905 the central equatorial Pacific. *Deep Sea Research Part II: Topical Studies in Oceanography*,
906 44, 2191. doi:10.1016/s0967-0645(97)00060-x

907

908 **Data Accessibility**

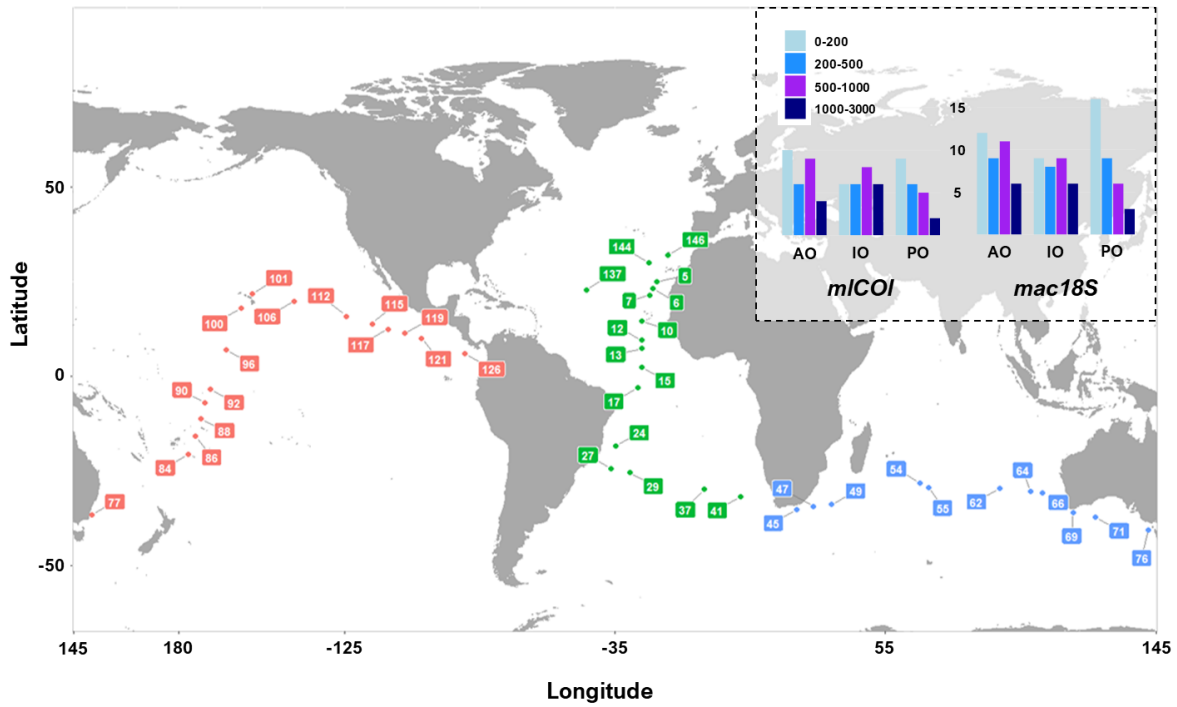
909 Raw sequence data and associated metadata are available on the NCBI SRA ([to be
910 completed upon acceptance]).

911 **Author Contributions**

912 XI and NRE designed research. OC, JC, EV, GC, EA, IM, and NRE performed research. JC, EA,
913 IM, CTM, JIG and NRE contributed new reagents or analytical tools. OC, JC, EV, EA and NRE
914 analysed the data. OC wrote the paper, with insightful contributions from EV, GC, XI and
915 NRE. All authors revised the manuscript and agreed with its publication.

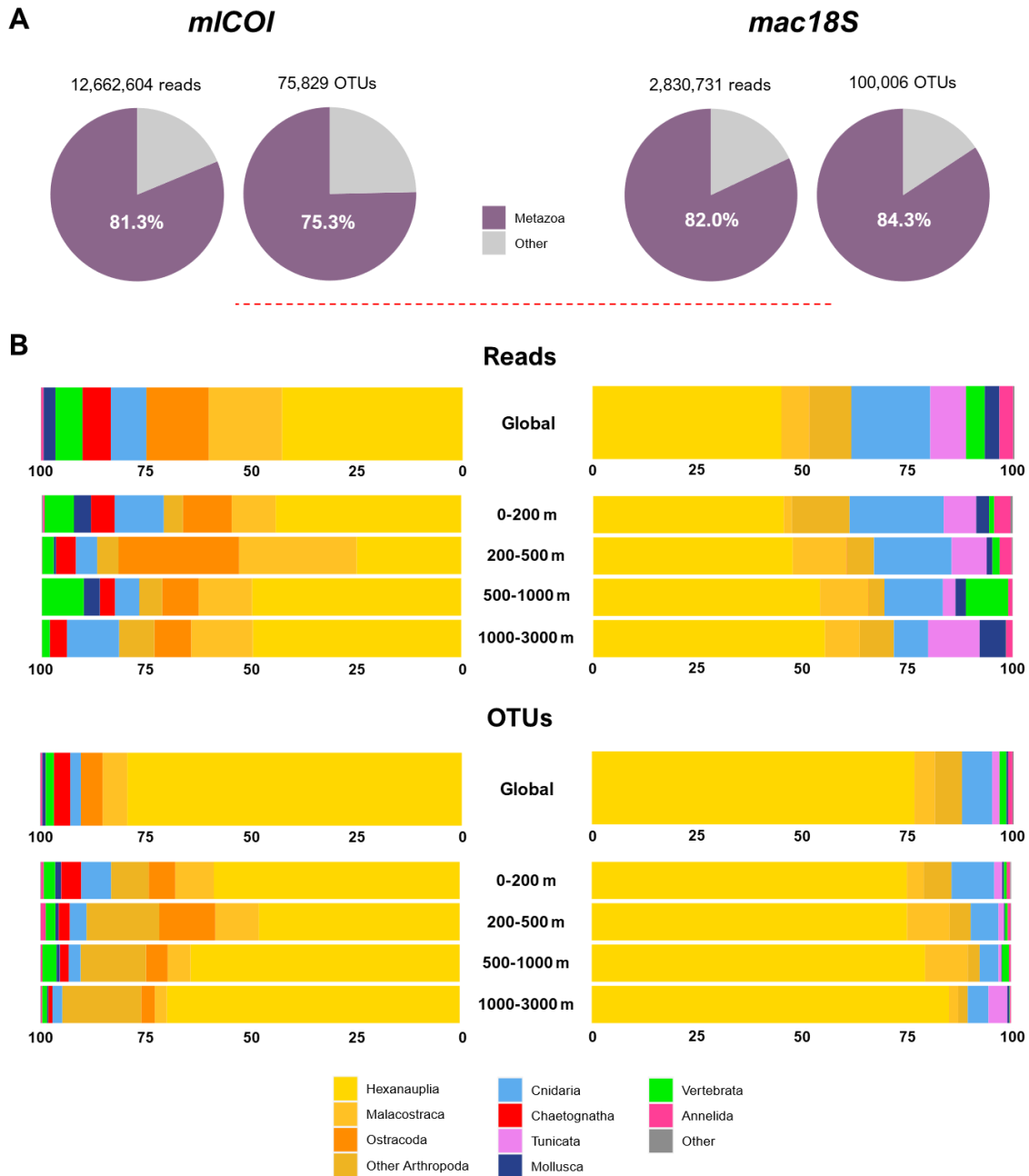
916 Tables and Figures (with captions)

917



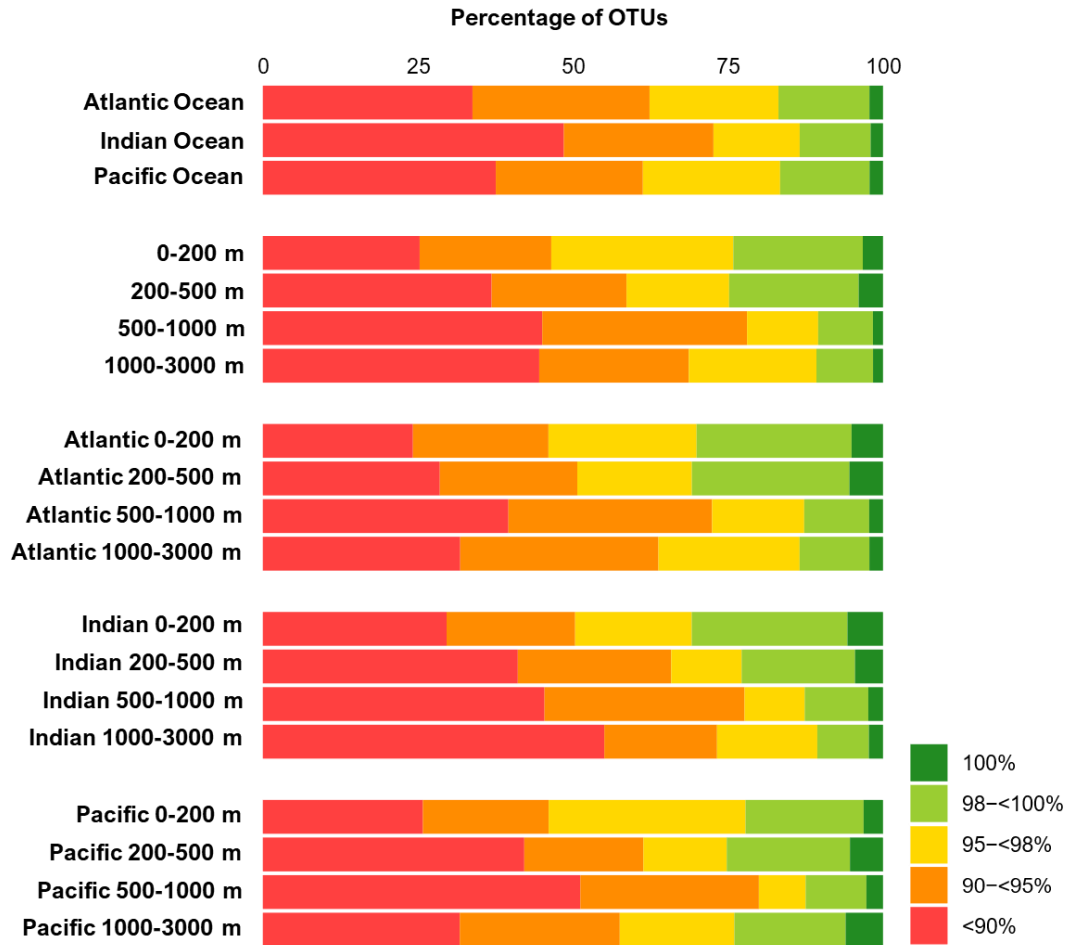
918

919 **Figure 1.** Location of the sampling stations of the Malaspina-2010 expedition from where
920 mesozooplankton samples were analysed in this study (map) and number of samples
921 analysed per depth range in the different oceanic basins for each marker (top right square).
922 AO: Atlantic Ocean, IO: Indian Ocean, PO: Pacific Ocean.



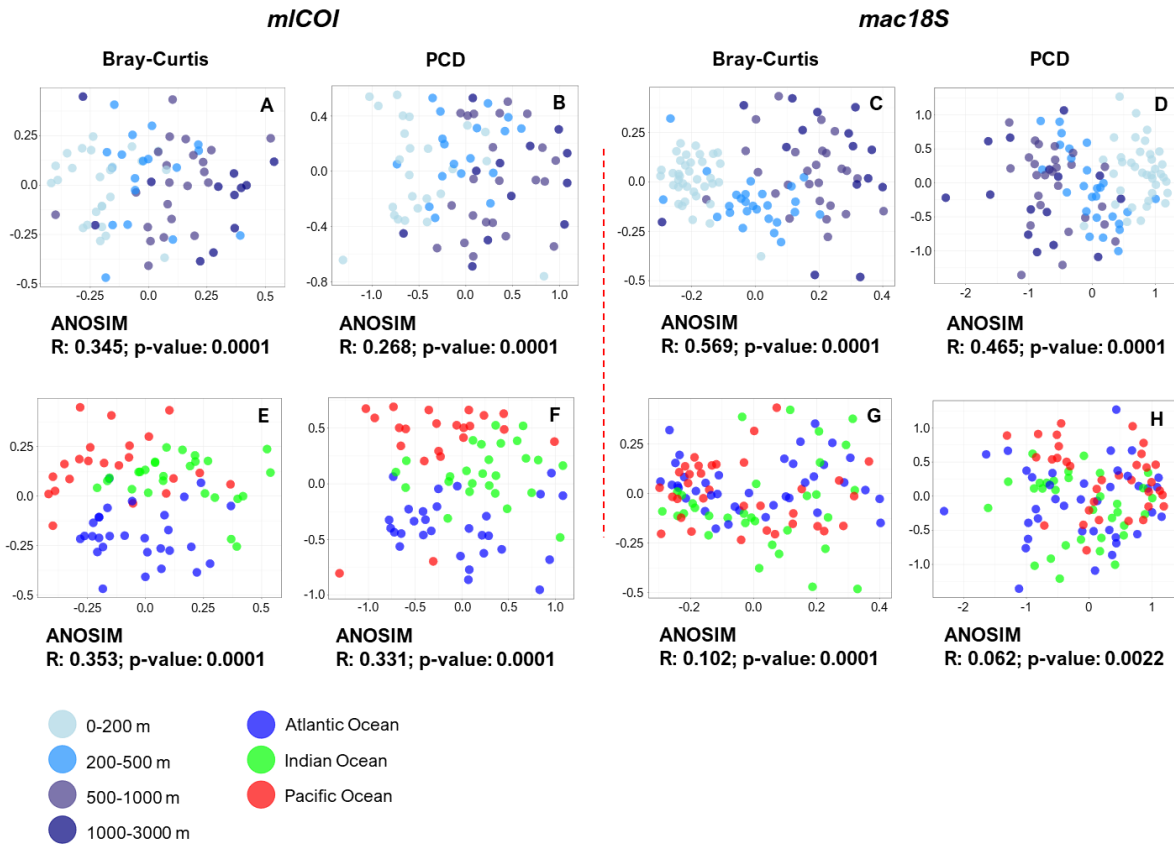
923

924 **Figure 2.** Overview of mesozooplankton taxonomic diversity in *mICOI* and *mac18S* datasets.
 925 **A:** Proportion of reads and OTUs assigned to Metazoa (Phylum level) and other (including
 926 unclassified, non-metazoan, and metazoan OTUs not assigned at Phylum). **B:** Proportion of
 927 reads and OTUs assigned to each metazoan Phyla and most abundant Classes within
 928 Arthropoda, globally and per depth range.



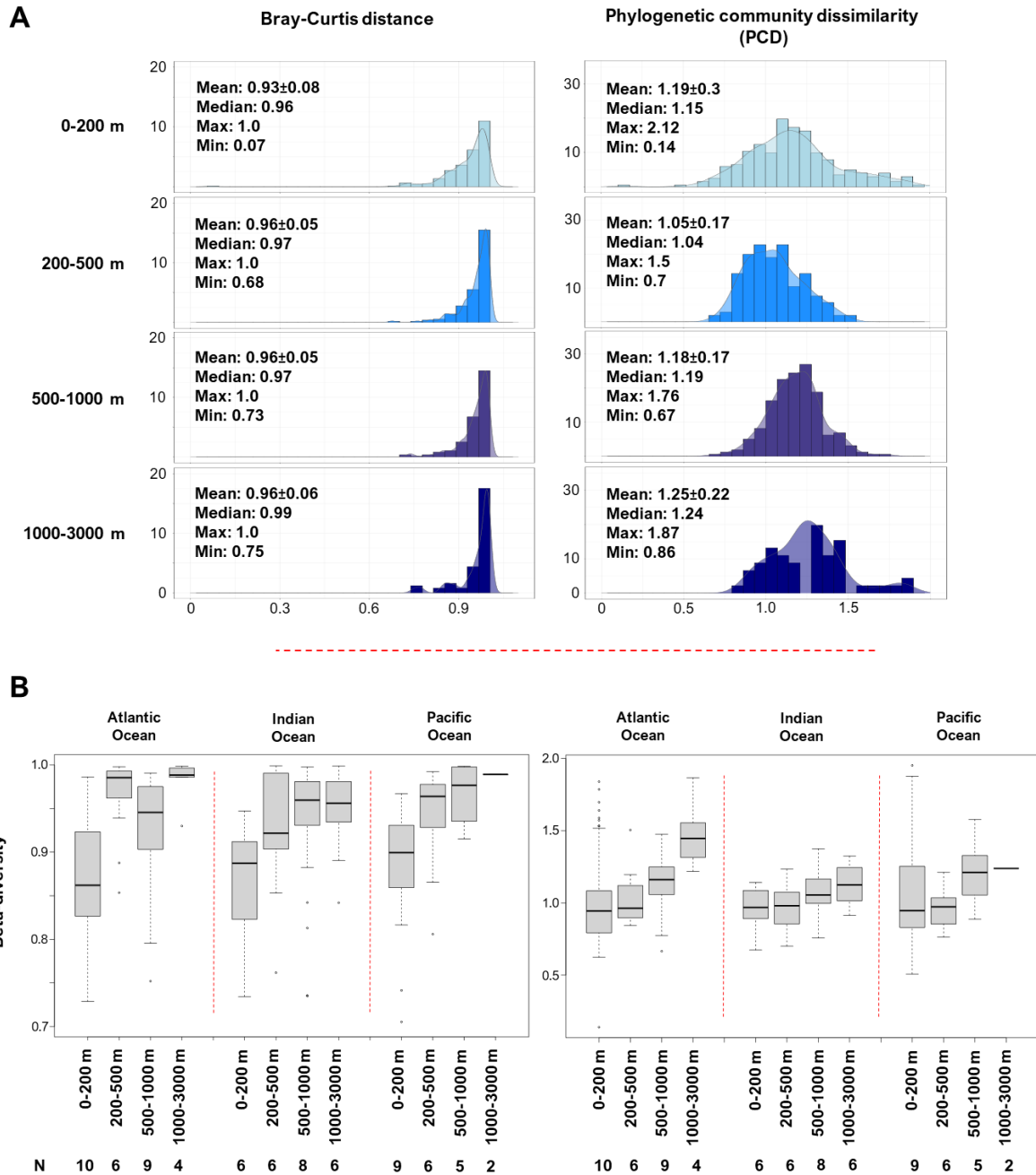
929

930 **Figure 3.** Percentage of *m/COI* OTUs with 100% (dark green), 98-100% (light green), 95-98%
 931 (gold), 90-95% (orange), and less than 90% (red) sequence similarity to any sequence of the
 932 MetaZooGene database for the Atlantic, Indian, and Pacific Oceans, for the four depth
 933 ranges under study, and for each combination of oceanic basin and depth range.



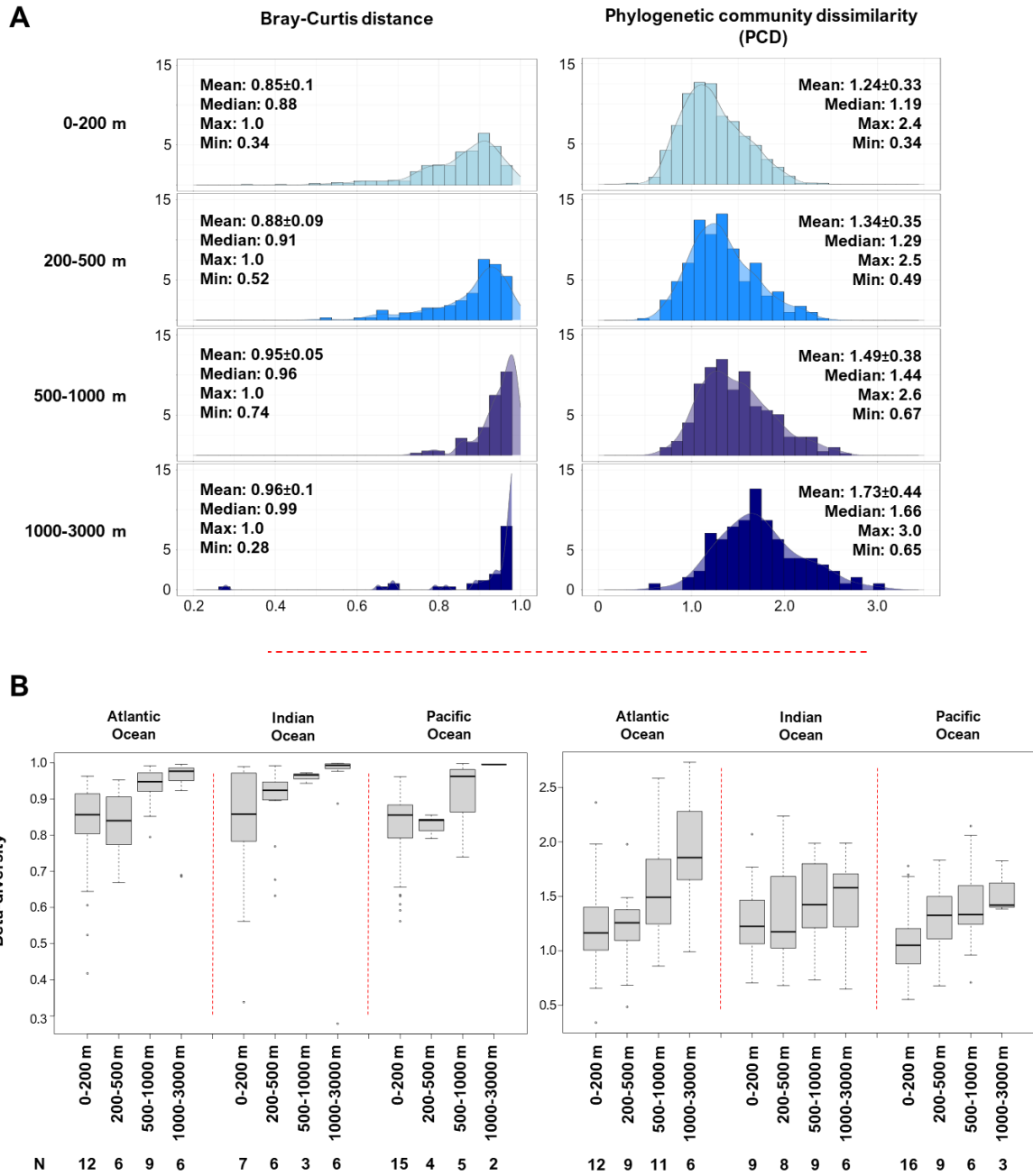
935

936 **Figure 4.** Ordination of mesozooplankton communities by NMDS (non-metric
 937 multidimensional scaling) analysis based on Bray-Curtis and PCD beta-diversity
 938 measurements for *mICOI* and *mac18S* datasets; plots A-D coloured by depth, plots E-H
 939 coloured by oceanic basin. Stress values of plots A and E: 0.247, B and F: 0.226, C and G:
 940 0.258, D and H: 0.214.



941

942 **Figure 5. A:** Histograms of beta diversity measurements based on Bray Curtis distances and
 943 PCD (phylogenetic community dissimilarities) between mesozooplankton communities
 944 from each depth range in the *m/COI* dataset. **B:** Boxplots showing the distribution of beta-
 945 diversity measurements (Bray Curtis and PCD) between mesozooplankton communities at
 946 each depth range from each oceanic basin separately. N indicates the number of samples
 947 considered in each boxplot.



948

949 **Figure 6. A:** Histograms of beta diversity measurements based on Bray Curtis distances and
 950 PCD (phylogenetic community dissimilarities) between mesozooplankton communities
 951 from each depth range in the *mac18S* dataset. **B:** Boxplots showing the distribution of beta-
 952 diversity measurements (Bray Curtis and PCD) between mesozooplankton communities at
 953 each depth range from each oceanic basin separately. N indicates the number of samples
 954 considered in each boxplot.

955 **Table 1.** ANOSIM test results regarding the grouping of mesozooplankton communities at
 956 the different oceanic basins by depth, at the different depths by oceanic basin, and the
 957 grouping of bathypelagic mesozooplankton communities by deep-water mass type (DWT;
 958 defined according to Catalá et al. (2015)). * p-value<0.1, **<0.05, ***<0.01, n.s. non-
 959 significant.

960

	<i>mICOI</i>				<i>mac18S</i>			
	Bray-Curtis		PCD		Bray-Curtis		PCD	
	R statistic	p-value	R statistic	p-value	R statistic	p-value	R statistic	p-value
Atlantic by depth	0.42	**	0.30	**	0.52	**	0.46	**
Indian by depth	0.30	**	0.19	**	0.44	**	0.29	**
Pacific by depth	0.60	**	0.29	**	0.82	**	0.70	**
0-200 by ocean	0.76	**	0.53	**	0.40	**	0.25	**
200-500 by ocean	0.22	**	0.39	**	0.27	**	0.11	n.s.
500-1000 by ocean	0.33	**	0.28	**	0.12	*	-0.04	n.s.
1000-3000 by ocean	0.27	†	0.15	n.s.	0.04	n.s.	0.05	n.s.
961 1000-3000 by DWT	0.51	*	0.79	**	-0.01	n.s.	0.41	**

962 **Table 2.** Results of Mantel test for each combination of marker, beta-diversity
 963 measurement, and depth, between mesozooplankton communities' distances and oceanic
 964 distances (log-transformed), environmental distances, and each environmental variable
 965 separately (temperature, salinity, oxygen, fluorescence, conductivity, and PAR—
 966 photosynthetically active radiation), and between oceanic and environmental distances. †
 967 p-value <0.1, *<0.05.

968

	<i>mICOI</i>								<i>mac18S</i>							
	Bray-Curtis				PCD				Bray-Curtis				PCD			
	0-200 m	200-500 n	500-1000 n	1000-3000 n	0-200 m	200-500 n	500-1000 n	1000-3000 n	0-200 m	200-500 n	500-1000 n	1000-3000 n	0-200 m	200-500 n	500-1000 n	1000-3000 n
Oceanic distance	0.58*	0.37*	0.48*	0.26*	0.45*	0.44*	0.46*	0.28*	0.21*	0.27*	0.13	0.37*	0.21*	0.19*	0.03	0.20*
Environmental distance	0.22*	0.32*	0.03	0.38*	0.35*	0.25*	0.23*	0.40†	0.15*	-0.01	0.18†	0.13†	0.05	0.21*	-0.2	0.35*
Temperature	0.19*	0.28*	-0.06	0.28†	0.13	0.18*	0.02	0.44*	0.11†	-0.12	0.24*	0.11	0.01	0.14*	-0.08	0.30*
Salinity	0.15*	0.18†	-0.05	0.36*	0.16†	0.19†	0.1	0.51*	0.04	0.11	0.17†	0.12	0.02	0.13†	-0.22	0.32*
Oxygen	0.20*	0.41*	0.35*	0.32*	0.43*	0.35*	0.41*	0.06	0.27*	0.17†	0.07	0.11	0.18*	0.25*	-0.04	0.29*
Fluorescence	-0.01	0.15	-0.08	0.2	0.22	0.26*	0.09	0.1	0.1	0.07	-0.03	0.09	0.01	0.23*	-0.2	0.22†
Conductivity	0.16*	0.26*	-0.07	0.30†	0.11	0.19*	0.02	0.46*	0.09	-0.11	0.24*	0.11	-0.001	0.12†	-0.12	0.32*
PAR	-0.04	-0.2	-	-	0.02	-0.24	-	-	-0.05	-0.06	-	-	-0.07	0.002	-	-
Oceanic vs environmental	0.26*	0.24*	0.17*	0.70*	0.26*	0.24*	0.17*	0.70*	0.16*	0.26*	0.12	0.66*	0.19*	0.21*	0.21*	0.68*

969

970